Uniaxial Ratcheting Behaviour of SA 508 Steel

A thesis submitted in partial fulfilment of the requirements for the degree of

Master of Technology

In

Metallurgical and Materials Engineering

Submitted by

Saurabh Kumar

Roll No. 210MM1154

Department of Metallurgical and Materials Engineering

National Institute of Technology Rourkela

Rourkela-769008

May-2012

Uniaxial Ratcheting Behaviour of SA 508 Steel

A thesis submitted in partial fulfilment of the requirements for the degree of

Master of Technology

In

Metallurgical and Materials Engineering

Submitted by
Saurabh Kumar

Roll No. 210MM1154

Under the Guidance of

Prof. K. DUTTA
Metallurgical & Materials Engineering Department,
National Institute of Technology Rourkela
Rourkela -769008

Dr. S.SIVAPRASAD (Senior Scientist)
Materials Science & Technology Division
National Metallurgical Laboratory
Jamshedpur- 831007

National Institute Of Technology
Rourkela

C E R T I F I C A T E

This is to certify that the thesis entitled, "**UNIAXIAL RATCHETING BEHAVIOR OF SA 508 STEEL**" submitted by **Mr. SAURABH KUMAR** in partial fulfilment of the requirements for the award of Master of Technology Degree in **METALLURGICAL AND MATERIALS ENGINEERING** with specialization in "**METALLURGICAL AND MATERIALS ENGINEERING**" at the National Institute of Technology, Rourkela is an authentic work carried out by him under our supervision and guidance.

To the best of our knowledge, the matter embodied in the thesis has not been submitted to any other University / Institute for the award of any Degree or Diploma.

Prof. K. Dutta
Dept. of Metallurgical and Materials Engg.
National Institute of Technology
Rourkela-769008

Dr. S.SIVAPRASAD (Senior Scientist)
Materials Science & Technology Division
National Metallurgical Laboratory
Jamshedpur- 831007

Date:

Place:

Acknowledgement

I avail this opportunity to express my heartfelt gratitude and regards to all those who help me a lot throughout my M.Tech course. First of all, I would like to convey my deep regards and thanks to my guide **Prof. Krishna Dutta,** Department of Metallurgical & Materials Engineering, National Institute of Technology, Rourkela who permits me to work at National Metallurgical Laboratory, Jamshedpur and always help me as friend and elder brother without his invaluable guidance, untiring efforts and meticulous attention at all stages during my project work I cannot complete my work.

I would also like to thank **Prof B.B.Verma** who always motivate me and enlighten me with his valuable suggestions.

I would also like to convey my deep regards to my co-supervisor Dr **. S.Sivaprasad, Principle Scientist,** National Metallurgical Laboratory, Jamshedpur, for his indebted help and valuable suggestions for the accomplishment of my experimentation and dissertation work.

I am also grateful to **Dr. N Narasaiah**, National Metallurgical Laboratory, and Jamshedpur who gave me suggestion on experimental work, carrier and general behavior. He also teaches us valuable managerial skills to manage a project. Other Scientist of same group like **Dr. H N Bar, Dr. J.K.Sahu, Dr. N Parida, and Dr. S. Tarafdar** also gave their valuable suggestion to bring out this thesis in time.

My sincere regards to, my friends like **Kaustav Barat, Anindya Das, Abhishek Chaturvedi and Pawan kumar,** for their co-operation during the period of work.

I am also thankful to **Mr. S. Hembram ,** Metallurgical & Materials Engineering, Technical assistants, for their help during the execution of SEM experiment.

Last but not the least special thanks to my **parents and family members** without whom support and motivation I cannot complete this course.

Saurabh Kumar

Contents

ABSTRACT

In piping materials, such as SA508 steel, used for pressurized heavy water reactors of nuclear power plants, ratcheting is manifested as a critical problem since it may alter the fatigue life of the said structure. Ratcheting is a type of strain accumulation which may occur from the cyclic loading conditions emanating from start-up and shut-down of the plant, variation in operating conditions or particularly in seismic events. It occurs due to asymmetric cyclic loading condition in low cycle fatigue domain. The nature of strain accumulation and associated fatigue life of a material may vary based on different loading parameters such as mean stress, stress amplitude, maximum stress, minimum stress, stress ratio and temperature. Studies on ratcheting behaviour for AISI 304 stainless steel, Cr-Mo steel, carbon steel, aluminium and Cu-alloys have been done by numerous researchers in past few years; although enough scope of work still exists to understand the phenomenon more precisely. It has been recognized that piping material like SA508 steel is prone to ratcheting, but no work is still reported in the literature regarding ratcheting behaviour of steel.

To start working with SA508 pressure vessel steel, the material is first characterized for its chemical composition, microstructural features, hardness and mechanical properties. The microstructure consists bainitic structure. Tensile tests are carried out at nominal strain rate of $1 \times 10^{-3} s^{-1}$ on 7 mm dia.

True stress control cyclic loading tests are carried out in room temperature environment, where effects of stress amplitude (σ_a) and mean stress (σ_m) on the ratcheting behaviour are examined. In one set of experiments, σ_m is varied keeping σ_a constant, while in a second set σ_m is kept constant and σ_a is varied. The chosen σ_m ranges from positive to zero to negative. An end criterion of the tests is doing cycling up to fracture. It is noted that the accumulation of ratcheting strain increases with increasing σ_m and σ_a while the other parameter is constant.

The increase in strain accumulation with increasing magnitude of stress amplitude can be explained with increasing width of stable hysteresis loop with increasing energy of deformation.

Keywords: Ratcheting, Stress amplitude, Mean stress, SA508 steel

LIST OF FIGURES

# # # #
#

# # # #
#

LIST OF TABLES

Page

# # # #
#

CHAPTER-1

INTODUCTION

1.1 Introduction

Ratcheting is a type of strain accumulation which occurs in engineering structures due to asymmetric cyclic loading conditions in low cycle fatigue domain. Asymmetric cyclic loading conditions may generate from start-up and shut-down of a plant, variation in operating conditions of structural members, or particularly to buried pressure vessel pipelines during seismic events. Pressure vessel piping materials, such as SA333 C–Mn steel, used for pressurized heavy water reactors of nuclear power plants, gets affected due to ratcheting; has become the research interest of several groups of researchers [1-3]. Ratcheting behaviour has also been in many other engineering materials such as: 304LN stainless steel [4], 1026 carbon steel [5], Elbrodur-NIB copper alloy [6] and 1070carbon steel [7] in the last two decades by several investigators. Study of ratcheting is manifested as a critical problem since it may alter the fatigue life of the assumed structure [8].

The nature of strain accumulation and associated fatigue life of a material may vary based on different loading parameters such as mean stress [9], stress amplitude [10], maximum stress [11], minimum stress [11], stress ratio [6,11] and temperature [9,12].It was observed that most of the investigations related to ratcheting are done with controlling the engineering stress. On the other hand very little information is available for true stress controlled ratcheting. In engineering stress control test, specimens are usually failed through necking rather than by initiation and growth. Therefore this investigation is primarily done by controlling the tests under true stress control are of more practical sense. It has been recognized that piping material like SA508 steel is prone to ratcheting, but no work is still reported in the literature regarding ratcheting phenomenon in this steel.

To start working with SA508 pressure vessel steel, the material was first characterized for its chemical composition, micro structural features, hardness and mechanical properties. Studies of ratcheting behavior of the steel were done by controlling true stress. The true stress control was adopted by adjusting various combinations of mean stress and stress amplitude during cyclic loading. The experiments were designed in such a manner that the loading parameters fall under constant mean stress with varying stress amplitude and constant stress amplitude with varying mean stress. All the tests were conducted up to fracture. Fractographic examinations were carried out on a set of representative fractured samples using scanning electron microscopy.

1.2Objectives of the present work

- To characterize the steel SA 508 steel for its microstructure, hardness and conventional mechanical properties.
- To study the effects of various combinations of mean stress and stress amplitude on the nature of strain accumulation during uniaxial ratcheting deformation.
- Fractographic examinations on fractured samples using scanning electron microscopy.

1.3 Lay out of the work

This thesis contains six chapters. The requirement of related experiments along with significance of the problem is described in **Chapter-1**. Literature background related to fatigue and subsequently ratcheting behavior of various materials are presented in **Chapter-2**. The information which is available in the literature generates many queries and provides the directions for further research. The present study has been inspired by the achievements of

the previous investigations. Details of test procedures material characterization, chemical composition analysis, microstructure analysis, hardness, test conditions and factors affecting tests have been discussed in **Chapter 3**. Obtained results on microstructures, hardness, conventional mechanical properties and ratcheting phenomenon of the investigated steel are discussed in **Chapter 4**. Conclusions derived from this work are summarized briefly in **Chapter-5** together with some proposed future work related to this area. All references cited throughout the thesis are compiled at **Chapter 6**.

CHAPTER -2

LITERATURE REVIEW

2.1 Fatigue:

When a material is subjected to repeated loading and unloading, nominal maximum stress values are less than the ultimate tensile stress limit, or may be below the yield stress limit, the material may fail due to progressive localized damage known as fatigue .It has become progressively more appropriate in the areas, such as automobiles, aircraft, compressors, pumps, turbines, etc., due to vibration and fluctuating load. Today it is often stated that fatigue accounts for at least 90 percent of all service failures due to mechanical causes [I, II]. Three basic factors are necessary to cause fatigue failure. These are:

ÅHigh value of maximum tensile stresses,

ÅLarge sufficient variation or fluctuation in the applied stress, and

ÅLarge number of cycles of the applied stress.

Some of the other variables, such as temperature, stress concentration, residual stresses, corrosion, overload, metallurgical structure, and combined stresses, which have a tendency to change the conditions for fatigue.

Although fatigue failures may seem to be abrupt, the process of fatigue fracture is progressive, beginning as mature cracks that grow during the service life of components. Sub-microscopic changes take place in the crystalline structure of metals and alloys under the action of repetitive low level load applications. These minute changes accumulate to lead to the formation of tiny microscopic cracks. The tiny cracks grow under cyclic loading into larger cracks. The larger cracks continue to grow until the stress in the remaining ligament becomes unsustainable, when sudden failure occurs. The growth history of fatigue cracks can

conveniently be sub-divided into three stages: crack initiation, incremental crack growth, and final fracture. [III]

Initiation of fatigue cracks usually occurs at free surfaces. This is because of the higher stresses and the higher probability of the existence of defects at these locations (for example, existence scratches, corrosion pits, bolted joints etc.). Even at highly-polished defect-free surfaces, fatigue cracks can initiate. According to W.A. Wood, these cracks initiate through repeated micro-plastic deformations which result in the formation of the ñintrusionsò and ñextrusionsò on the surface [I]. Formation of micro-cracks may start from these intrusions, as these can act as local stress concentration sites. Different stages exist in fatigue crack initiation and propagation. The crack grows in stage I at a tilt, in a crystallographic fashion. Gradually it deflects into a Stage II crack when a striation forming mechanism dominates. Fatigue crack propagation occurs through repeated crack tip blunting and sharpening effects which are in turn caused by micro-plastic deformation mechanisms operating at the crack tip. It occurs over a long period of time; the fracture surface may contain characteristic markings which are called ñbeach markingsò or ñclamshell markingsò. These markings, which are recognizable even by naked eye, reflect the occurrence of different periods of crack growth. On the other hand, there are extremely fine parallel markings, at intervals of the order of 0.1 εm or more called ñstriationsò, which represent the crack growth due to each individual loading cycles and can seen at higher magnifications using electron microscopes.

Generation of striations occur from two primary mechanisms: alternating slip and crack tip blunting and re-sharpening, as schematically shown in Fig. 2.1.

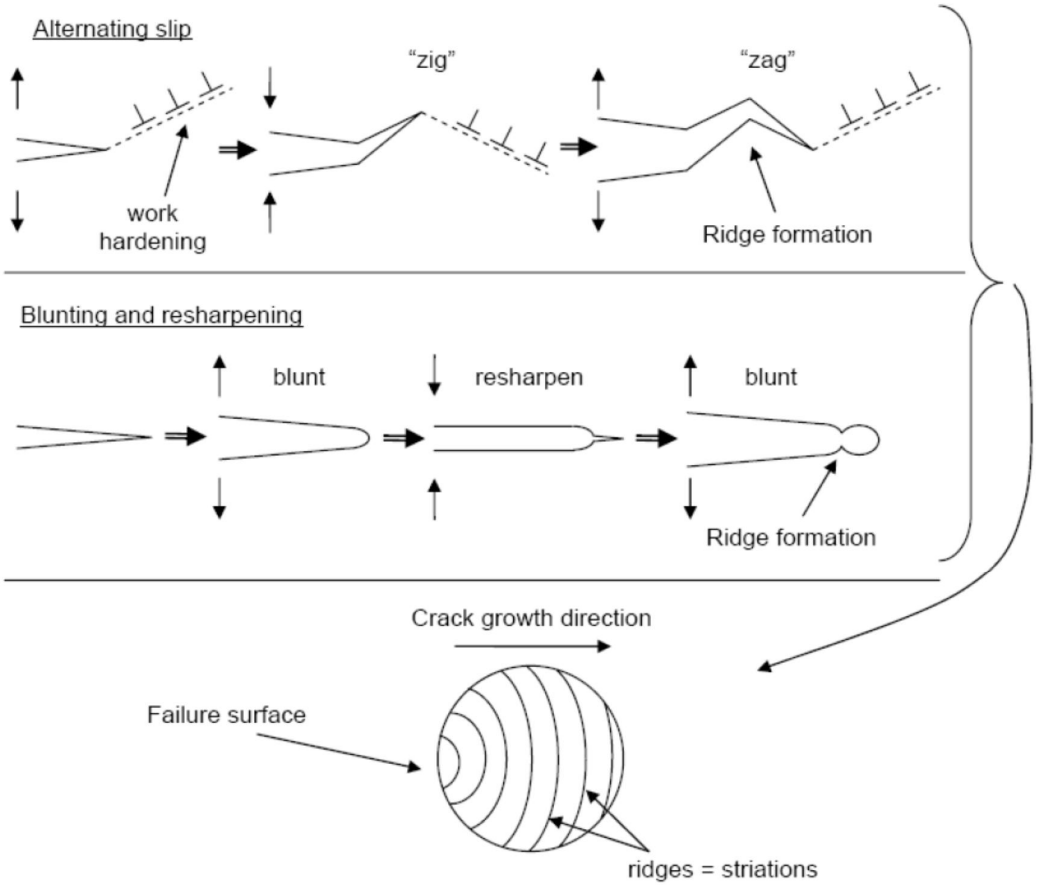

Figure2.1 Schematic representation of striation formation during fatigue crack growth.

When the crack tip plasticity is limited alternating slip occurs, so that dislocations only move on a small number of parallel planes. As the dislocations are produced at the crack tip under load, they will tend to pile up close to the crack tip, resulting in localized work hardening. This work hardening tends to embrittle the material, making it easy for the crack to grow on the slip plane. As the crack grows, new slip planes are activated, and the process is repeated as illustrated above. As the slip planes alternate, the crack follows a ñzigzagsò path and sharp ridges are formed on the failure surface. Crack tip blunting and re-sharpening occurs in materials capable of more generalized yielding at the crack tip. Upon loading, the

initially sharp crack will blunt due to plastic deformation. Small crack length is increase due to blunting. When the crack is unloaded, the elastic stress field around the plastically relaxed crack tip will cause the crack to resharpen. Reloaded the crack, blunting is again, leave a ripple on the surface.

Further on, in Stage III, static fracture modes are superimposed on the growth mechanism, till finally it fails catastrophically by shear at an angle to the direction of growth. Fig. 2.2representsaschematic the various stages of fatigue crack growth.

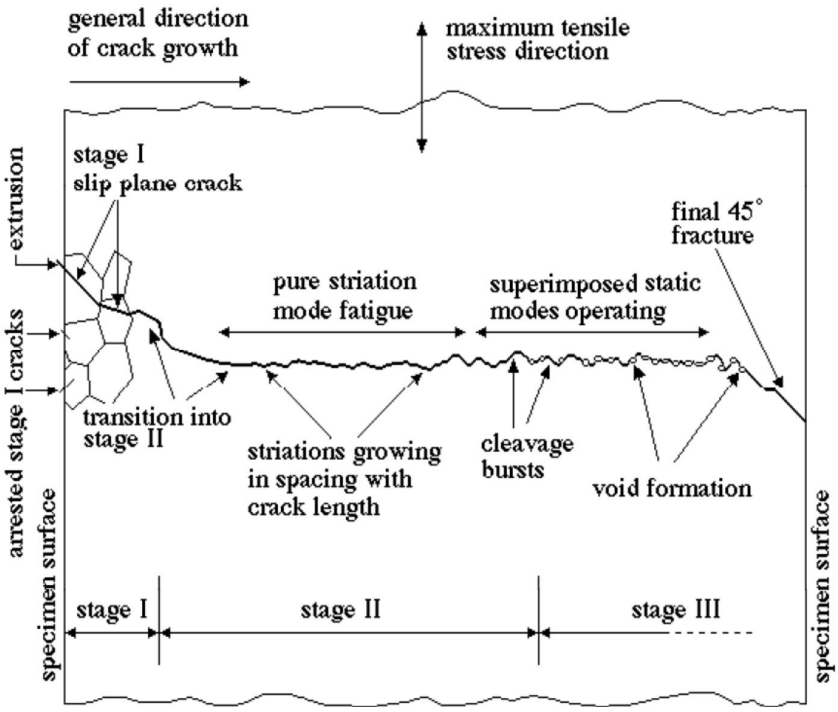

Figure 2.2 Schematic representations of the various stages of fatigue crack growth

2.2 Different nomenclature to describe test parameters

Different nomenclature is there in fatigue literature which can be enlisted as follows:

- Stress range (æσ) = σ_{max}ï σ_{min}
- Stress amplitude (σ_a) = (σ_{max}ï σ_{min}) /2
- Mean Stress (σ_m) = (σ_{max} + σ_{min})/2
- Stress ratio (R) = σ_{min} ùσ_{max}
- Amplitude ratio (A) = σ_a/σ_m = (1ï R)/(1+R)

2.3Types of cyclic loading

As can be seen in the figures given below, cyclic loading may be of different natures. These are:[I]

Completely reversed cycle: In this type of cyclic loading, maximum and minimum stresses are equal. It is symmetric loading ($\mathring{u}_m$ = 0). Tensile stress is considered positive and compressive stress is negative (Fig 2.3(a)).

Asymmetric loading: repeated stress cycle in which the maximum stress $\mathring{u}_{max}$ and $\mathring{u}_{min}$ are not equal. Both are in tension, but some time it may be tension and compression both. This is known as asymmetric loading ($\mathring{u}_m$ Í 0, Fig 2.3(b)).

Random stress cycle: this type of stress cycle generated in a part such as an aircraft wing which is subjected to periodic unpredictable load due to gusts (Fig 2.3(c)).

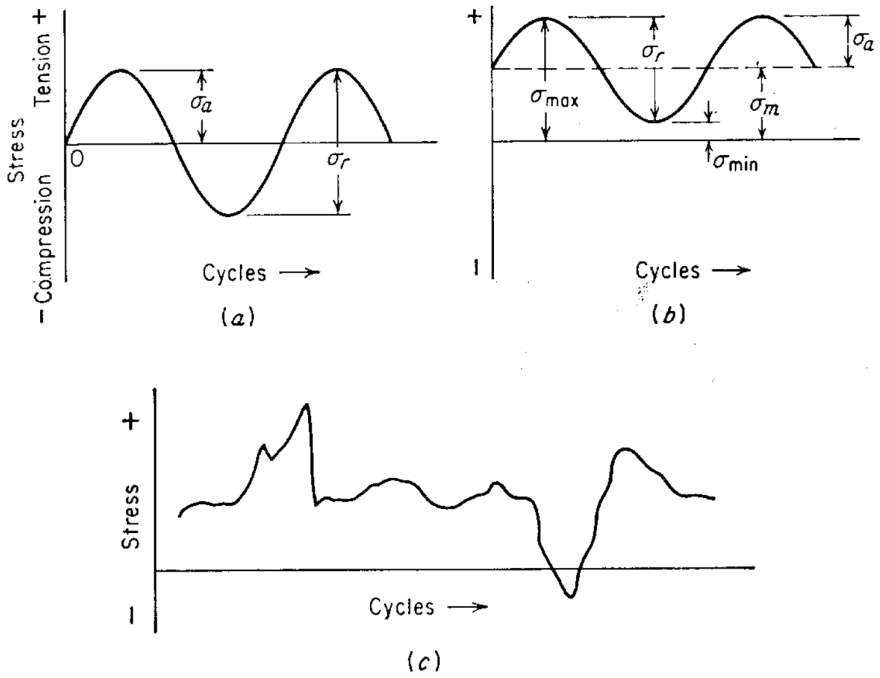

Figure 2.3(a) completely reversed stress cycle (b) asymmetric stress cycle (c) Random stress cycle.

2.4High Cycle Fatigue and Low Cycle Fatigue:

There are two types of fatigue failure divided on the basis of total life of a component are low and high cycle fatigue (LCF and HCF).

2.4.1 High Cycle Fatigue

In HCF, the life is usually characterized as a function of the stress range applied, and the components fail after a high numbers (Usually higher than 10^6 cycles) of cycles at a relatively

Low stress (Usually less than 30 % of yield stress), and the deformation experienced is primarily elastic [I]. High cycle fatigue must be considered during design of automobiles, aircraft, compressors, pumps, turbines, etc. where vibration occur. HCF test is done at frequency always greater than 1 KHz.

The high cycle fatigue is defined by the Basquin equation

$N\sigma_a^p = C$.....1

Where $\mathring{u}_a$ is the stress amplitude and p and c are empirical constants

The S-N Curve:

The basic method of presenting engineering fatigue data is by means of the S-N curve Fig. 2.4, a plot of stress $\mathring{u}$ against the number of cycles to failure N. A log scale is almost always used for N. The value of stress that is plotted can be $\mathring{u}_a$, $\mathring{u}_{max}$, or $\mathring{u}_{min}$. The nominal stresses values are usually used means there is no adjustment for stress concentration. The S-N relationship is determined for a specified value of $\mathring{u}_m$, R or A.

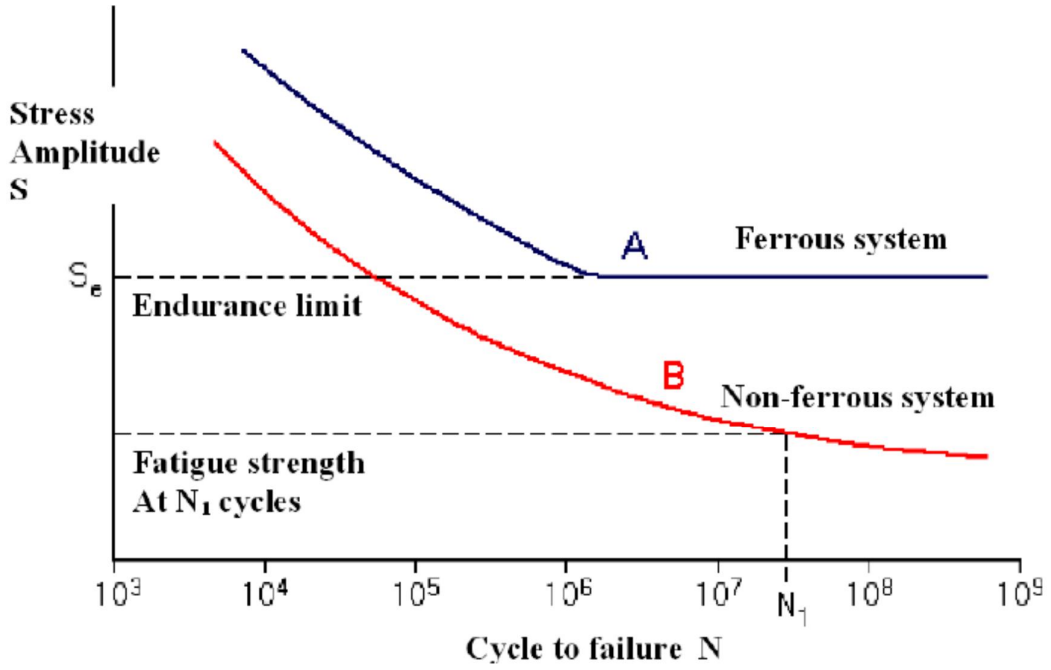

Figure2.4 Schematic representation of S-N curve: (A) Ferrous system; (B) Non-ferrous system

For determinations of the S-N curve, the usual procedure is to test the first specimen at a high stress where failure is expected in a fairly short number of cycles, which is generally about two-thirds of the static tensile strength of the material. The test stress is decreased for each succeeding specimen until one or two specimens do not fail in the specified numbers of cycles, which is usually at least 10^7 cycles.

The highest stress at which a run-out (non-failure) is obtained is taken as the fatigue limit. For materials without a fatigue limit, the test is usually terminated for practical considerations at a low stress where the life is about 10^8 or $5x10^8$ cycles. The S-N curve is usually determined with about 8to 12 specimens.[III]

2.4.2Low Cycle Fatigue

The low cycle fatigue, where life is characterized as a function of the strain range and the component fails after a small number of cycles at a high stress, where largely plastic deformation is obtain. In thermal origin strain controlled cyclic loading is found, because a component expands and contracts in the operating temperature. Low cycle fatigue must be considered during design of nuclear pressure vessels, steam turbines and other type of power machineries. Low cycle fatigue test is done at frequency less than 1 Hz.[I]

The usual way of presenting low-cycle fatigue test results is to plot the plastic strain range $\Delta\varepsilon_p$ against N. This graph is plotted in log-log co-ordinates.

The behaviour of low cycle fatigue is described by Coffin-Manson relation, which is

$$\Delta\varepsilon_p/2 = \varepsilon_f(2N)^c \quad \text{.....2}$$

Where,

$\Delta\varepsilon_p/2$ = plastic strain amplitude

ε_f = fatigue ductility coefficient defined by strain intercept at 2N = 1

2N = number of strain reversals to failure

C = fatigue ductility exponent, which varies between -0.5 to -0.7 for many metals

2.5 Effect of Mean Stress on Fatigue

Much of the fatigue data in the literature have been determined for conditions of completely reversed cycles of stress, $\mathring{u}_m = 0$. Still, situation is normally met in engineering field where an alternating stress and a superimposed mean, or steady, stress. There are more feasible methods to determining an S-N diagram where $\mathring{u}_m = 0$. Fig 2.5 shows the mean stress in relating the fatigue endurance limit. All these relationships show that the alternating stress amplitude required for fatigue endurance limit gradually decreases with increasing of the mean stress.

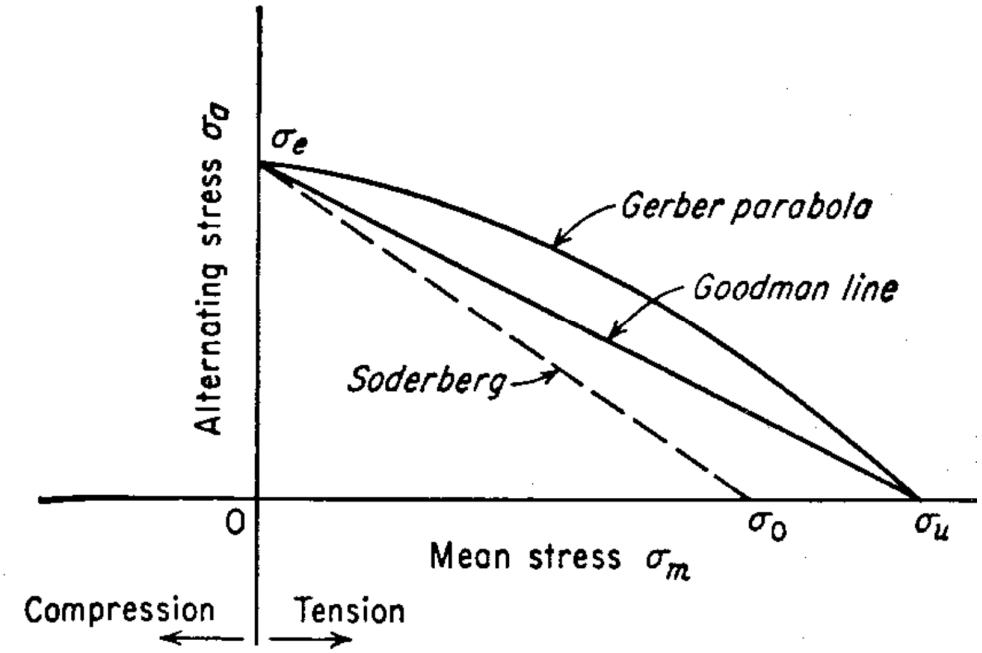

Figure2.5 Effect of mean stress on alternating stress amplitude at fatigue endurance

The mathematical formulations for the various curves in Fig2.6 are:

Gerber: $(\mathring{u}_a/\mathring{u}_e) + (\mathring{u}_m/\mathring{u}_u)^2 = 1$ é é é é é é ..é é é é é é é é é é é é é é é é .... (3.a)

Goodman: $(\mathring{u}_a/\mathring{u}_e) + (\mathring{u}_m/\mathring{u}_u) = 1$ é .. (3.b)

Soderberg: $(\mathring{u}_a/\mathring{u}_e) + (\mathring{u}_m/\mathring{u}_y) = 1$ é . (3.c)

2.6Fatigue life prediction through different approach

2.6.1 Approach based on Stress

Wohler was the first researcher who studies on metal fatigue using the stress based approach in 1871 on rotating axles [14]. And Basquin was proposed in 1910.

True stress amplitude $\mathring{u}_a$ = æů/2 is used as the damage parameter instead of engineering stress.

Basquin Relationship: $\mathring{u}_a = \mathring{u}_f (2N_f)^b$

Where $\mathring{u}_f$ is the fatigue strength coefficient and b is the fatigue strength exponent. Fatigue strength exponent b, varies from-0.05 to-0.15. Also fatigue strength exponent b, can be calculated from strain hardening exponent n.

$b = \frac{\square\square}{\square\square\square\square}$ é . (4)

If we take account the effect of mean stress then Basquin Relation will be

$\mathring{u}_a = (\mathring{u}_f - \mathring{u}_m) (2N_f)^b$ é ..(5)

Approach based on Stress is mostly applicable to the high cycle fatigue region where the strain is essentially elastic.

2.6.2 Approach based on strain

The approach based strain was basically introduced for thermal and low cycle fatigue. This approach is popular for fatigue life estimation.

Coffin-Manson equation can be written as

$æ\varepsilon_p/2 = (\varepsilon_f).(2N_f)^c$

Where ε_f is the fatigue ductility coefficient which corresponds to the plastic strain at one reversal ($2N_f = 1$) and c is the fatigue ductility exponent. Fatigue ductility exponent c, varies from -0.4 to -0.8. Also fatigue ductility exponent c, can be calculated from strain hardening exponent n.

$$C = \frac{-1}{1+5n} \text{.....é é é é é é é é é é é é é é é é é é é .....é é é é é é é é .} \quad (6)$$

The mean strain effect in the low cycle fatigue can be accounted for by modifying the Coffin-Manson equation as

$æU_p/2 = (U_m ï U_p)(2N_f)^c$.....(7)

Where U_m is the mean strain.

Under condition of strain cycling cyclic life in terms of reversals to failure is expressed by Coffin-Manson and Basquin relationship

$æU_t/2 = æU_e/2 + æU_p/2 = (\sigma_f/E).(2N_f)^b + (\varepsilon_f).(2N_f)^c$.

Fig 2.6 shows the strain-life plots according to the above relationship. From this equation it is possible to determine the transition life ($2N_f$) and also the transition strain for the changeover between HCF and LCF.

It is found from Fig 2.6 that while below transition life plastic strain component predominates and above transition life elastic strain component predominates.

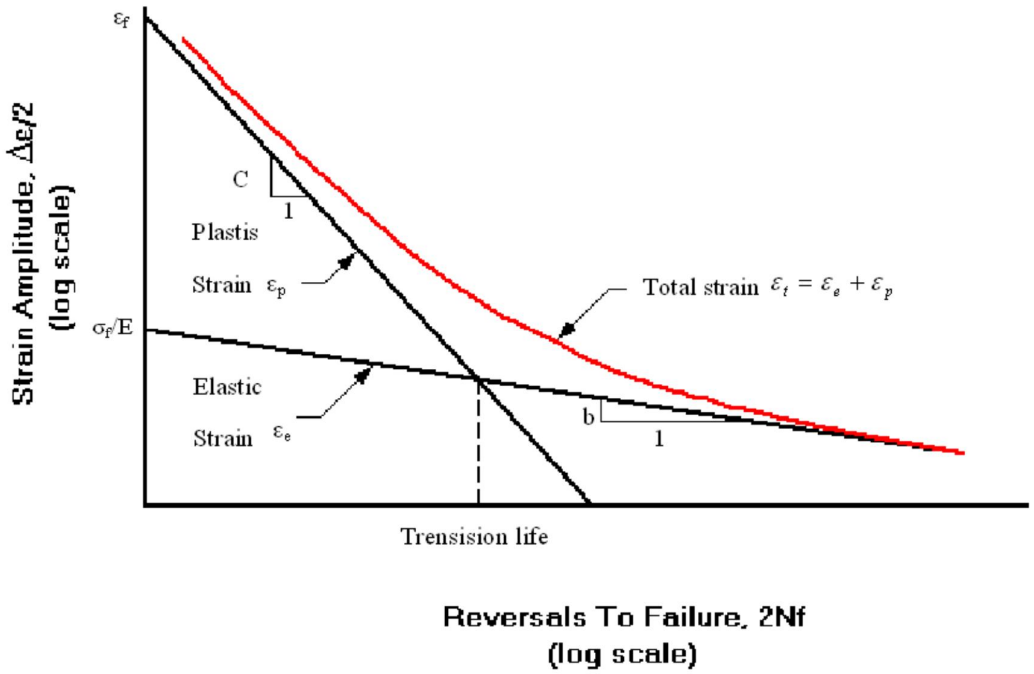

Figure2.6 Coffin-Manson and Basquin Plot.

2.7 Cyclic deformation behavior on different material

Response of Material deviates from that of the monotonic, once a reversed plastic deformation takes place. When a smooth solid specimen is subjected to one of the loading programme shown in Fig 2.7.

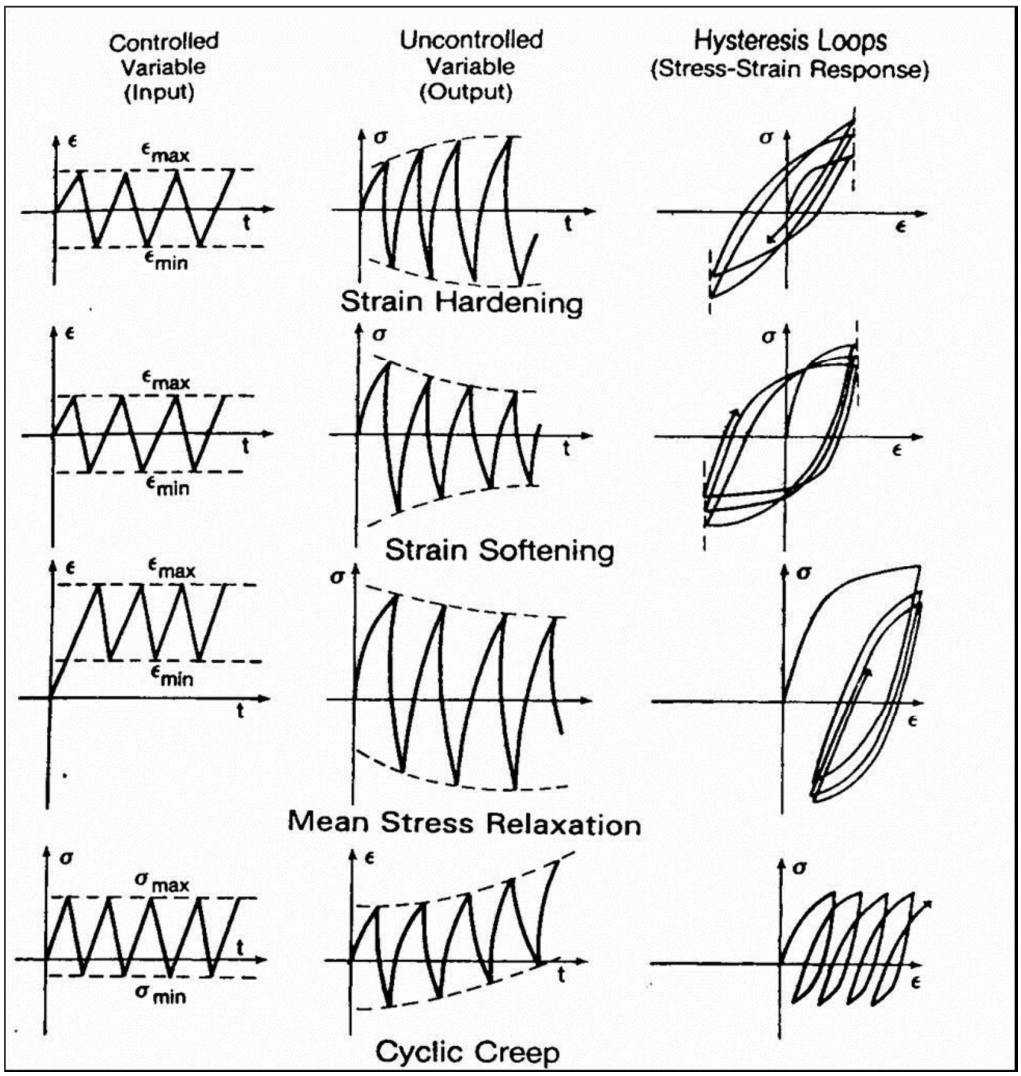

Figure 2.7 Schematic responses to various modes of cyclic input variables (deformation or stress controlled tests

To dislocation glide is generally increased, thus requiring higher stresses to continue the deformation. The cyclic important characteristics including cyclic mean stress relaxation hardening or softening, cyclic creep deformation (defined as ratcheting in the current investigation), rate dependency and memory effect. In the case where strain controlled tests is fully-reversed, the material retort initially few cycles it varies with the number of and later stabilizes. Lefebvre et.al studied the stress-strain response of pearlitic- ferritic steel (ASTM A-516 Gr. 70) [14]. It indicates strain-softening phenomena, i.e. the uncontrolled stress decreases with increasing number of cycles until a saturated state is achieved. It should be noted that at higher strain range ranges this steel hardens, i.e. uncontrolled stress increases with increasing number of cycles until it reaches a stable state. This type of activities is commonly observed for the low alloy carbon steels. During cyclic deformation the mobile segment of dislocation is reduced, leading to the formation of different obstacle structure. The resistance hardening rate is smaller at low strain amplitudes than at higher ones. For fully-reversed stress-controlled loading, it observes that strain hardening or softening similar to the strain-controlled condition. The plastic strain decreases with the number of cycles and reaches stable state for strain hardening material. The reverse occurs for strain softening material. When a mean stress is present, the response is rather complicated. For example, in the case of tensile mean stress, creep is observed under stress controlled condition which is shown above in Fig. 2.7. The ratcheting strain (cyclic creep strain) increases with increasing number of cycles.

It has been seen that the cyclic stress-strain curve differs from that of the monotonic curve in several aspects. First there is transition accompanied by either strain softening or hardening with respect to monotonic curve. A saturated state is subsequently reached. However the transient response depends on the test control mode, i.e. deformation (strain) or load (stress) control, and prior history of deformation.

2.8 Ratcheting

Ratcheting is the event of progressive accumulation of permanent deformation when any component is subjected to cyclic loads in the elastic-plastic strain range under stress controlled fatigue with non-zero mean stresses. Due to accumulation of plastic strain material will finally lead to a shakedown, or a constant rate of ratcheting or very large ratcheting strains ultimate to failure of the material [15]**.**It is low cycle fatigue domain responses. Ratcheting is important in designing and life evaluation of the structural components endured in cyclic loading. Ratcheting strain is a secondary strain produced under asymmetrical cyclic stressing, and has a great dependence on loading conditions and loading history. Other factors, such as ambient temperature and non-proportionality of loading path, have significant effects on ratcheting.

Different types of structures that are subjected to cyclic loading where the maximum stress exceeds the elastic limit of the materials used. For design and analysis of these types of structures, or materials accurate knowledge of ratcheting response is critical as ratcheting can lead to catastrophic failure of the structures. Even for structures that are designed to be within the elastic limit, plastic zones may exist at discontinuities or at the tip of cracks. The fatigue cracks can initiate at these plastic zones.

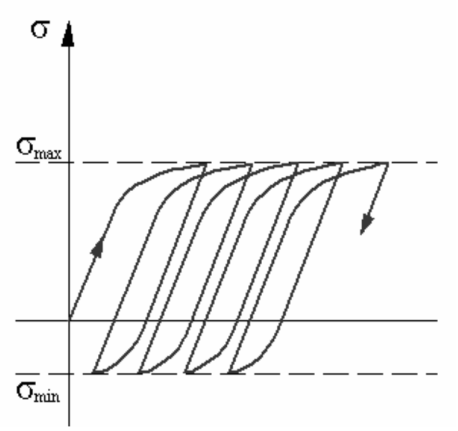

Figure 2.8 Ratcheting phenomenon

The ratcheting phenomenon is defined as a cycle-by-cycle accumulation of plastic strain with the application of cyclic load characterized by constant stress amplitude with none zero mean stress. After a sufficient number of cycles, the total strain (displacement) become so large that the original shape of the structure is altered, thereby making the structure unserviceable. The typical repetitive loading for ratcheting is shown in Fig. 2.8 [16].

The axial ratcheting strain ε_r is defined as fig 2.8

$$\varepsilon_r=\frac{1}{2}(\varepsilon_{min}-\varepsilon_{max}) \quad (8)$$

Where ε_{max} is the maximum of axial strain in each cycle, ε_{min} is the minimum axial strain. The axial Ratcheting strain rate is defined as the increment of ratcheting strain ε_r in each cycle and denoted dŮ/dN[9].

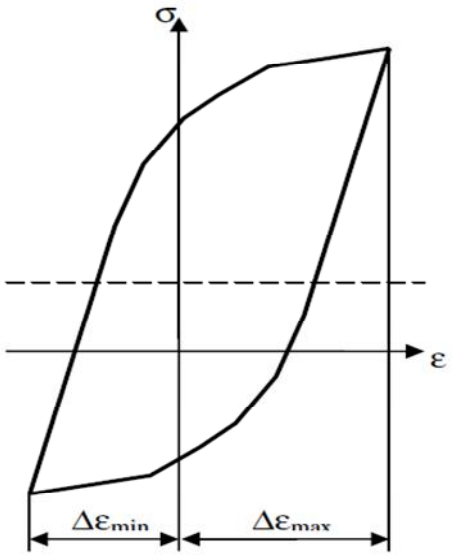

Figure 2.9 Peak stress and strain

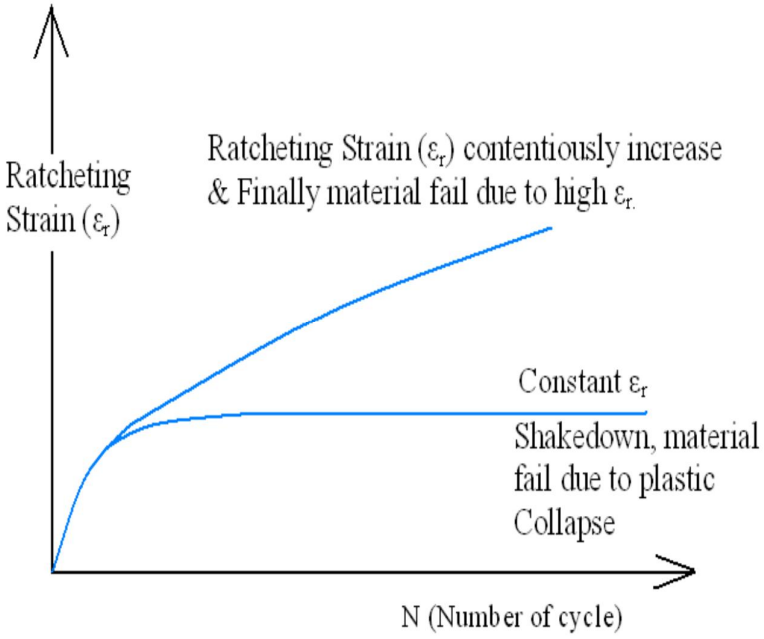

Figure2.10 Plot of ratcheting strain $\varepsilon_r$vs.number of cycle (N).

In the above Fig 2.10 we plot ratcheting strain $\varepsilon_r$vs. Number of cycles (N). If ratcheting strain ε_r increase continuously with number of cycle (N) that indicates, plastic strain accumulated with time and material is finally failed due to high plastic strain. If ratcheting strain ε_r first increase with number of cycle (N) then comes to a constant value that indicates that in first portion of the curve plastic strain accumulated with time then stops, so material do not fail due to ratcheting.

2.8.1 Shakedown

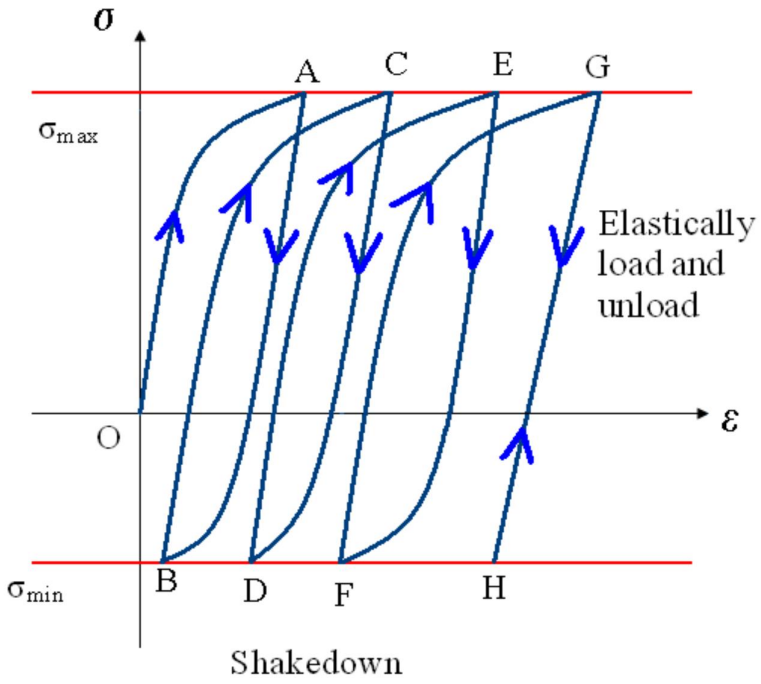

Figure2.11 Elastic shakedown

With occurrence of structural shakedown, the dissipated energy in the whole structure remains bounded after initial plastic flow and the structure respond in the purely elastic manner to the applied variable load [12].

2.8.2 Mean stress Relaxation

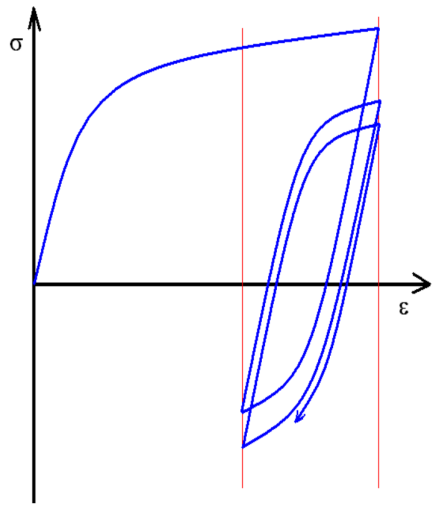

Figure2.12 Relaxation of mean stress

Relaxation of mean stress happens when we do an unsymmetrical strain experiment, as shown in Fig 2.12 for unsymmetrical strain experiment, a mean strain is introduced. Mean strain cause mean stress. So at the initial cycle a mean stress is introduced during unsymmetrical strain experiment .But as the cycling proceeds mean stress will relax and tends to zero.

2.9 Strain accumulation during ratcheting-effect of different factors:

There are different parameters which affect the strain accumulation during ratcheting. These parameters can be enlisted as:

- Mean stress,
- Stress amplitude,
- Maximum stress,
- Minimum stress,
- Stress ratio,
- Stress rate.
- Temperature,
- Characteristics of material.

2.9.1 Effect of mean stress and stress amplitude

Mean stress and stress amplitude are the most important parameters that affect the accumulation of strain during ratcheting; but most dominating is the mean stress [16].Many researchers have reported that strain is accumulated in presence of positive or negative mean stress. Kang et al. [9] have shown that strain accumulation increases with increasing mean stress at constant stress amplitude (Fig. 2.13) and varying stress amplitude with constant mean stress for SS304 material (Fig.2.14).

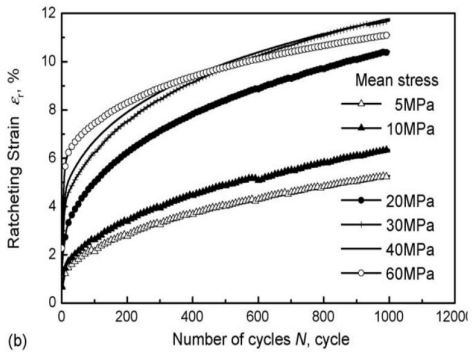

Figure 2.13 curves of ratcheting true strain vs. number of cycles with various mean stresses

.

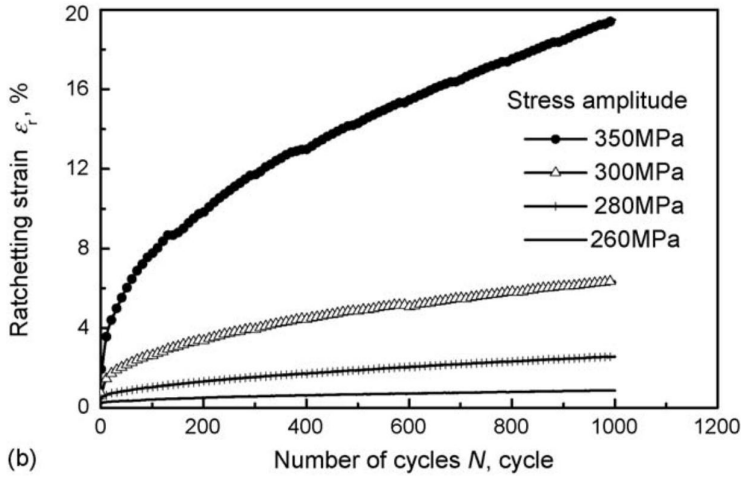

Figure 2.14 curves of ratcheting true strain vs. number of cycles with various stress amplitude.

In true stress controlled fatigue test Paul et. al [3], Sivaprasad et. al [2] found ratcheting strain varies directly with the stress amplitude at constant mean stress, which is explained by the plot shown in Fig.2.15 In case of constant stress amplitude, both ratcheting life and strain accumulation is increasing with tensile mean stress and strain accumulation paths are mirror of each other for tensile and compressive mean stress of equal magnitude.

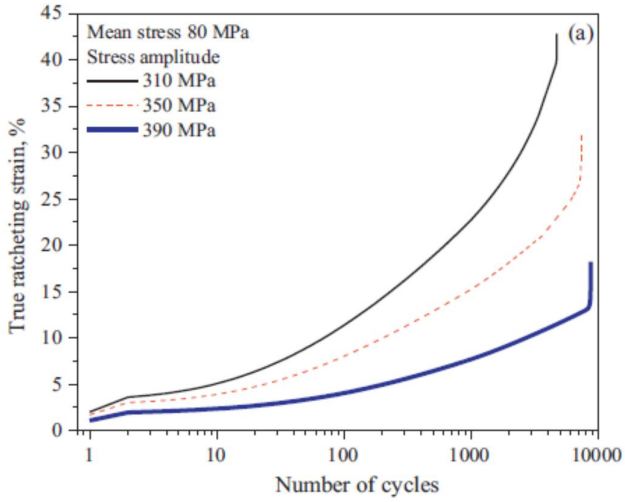

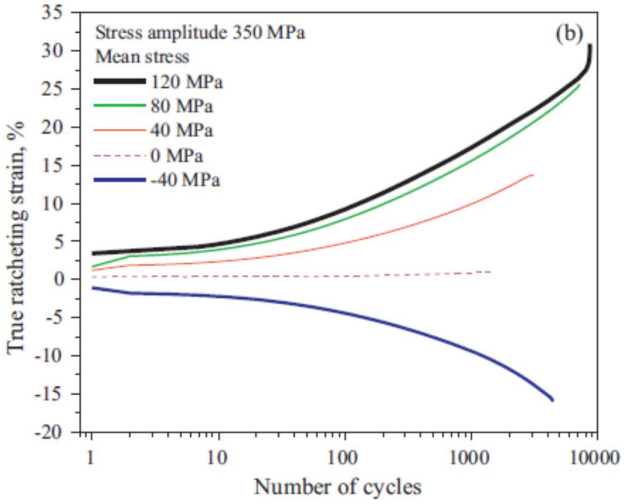

Figure2.15 True ratcheting strain as a function ofnumber of cycles (a) for constant mean and varying stress amplitude (b) for constant stress amplitude and varying mean stress.

Chen et. al [17] have reported that ratcheting strain and ratcheting strain rate of 63Sn37Pb increased with increasing stress amplitude or mean stress respectively and also shown that accumulation of ratcheting strain rate was very responsive to the applied cyclic stress rate. Several other researchers have found that ratcheting strain depends on both mean stress and stress amplitude.[18, 19].

2.9.2 Effect of cyclic hardening/softening features

Accumulation of ratcheting strain as well as fatigue life of the materials depends on the cyclic hardening/softening features of the materials. Yung-Chuan Chiou [20] studied the ratcheting behaviour of AISI 304 stainless steel, the cyclic stress response curves obtained for AISI 304 stainless steel exhibit either an initial cyclic hardening followed by softening, or continuous

Cyclic softening to fracture. Kang et al. [9] studied the ratcheting behaviour of 25CDV4.11 steel and SS304 stainless steel. 25CDV4.11 steel features cyclic softening outstandingly and SS304 stainless steel characteristics cyclic hardening apparently which is shown in Fig 2.16 When the material show cyclic softening behaviour, i.e., 25CDV4.11, accumulation of ratcheting strain increases with cycles, no shakedown of ratcheting takes place and the material finally fails due to the increasing ratcheting strain in spite of load conditions.

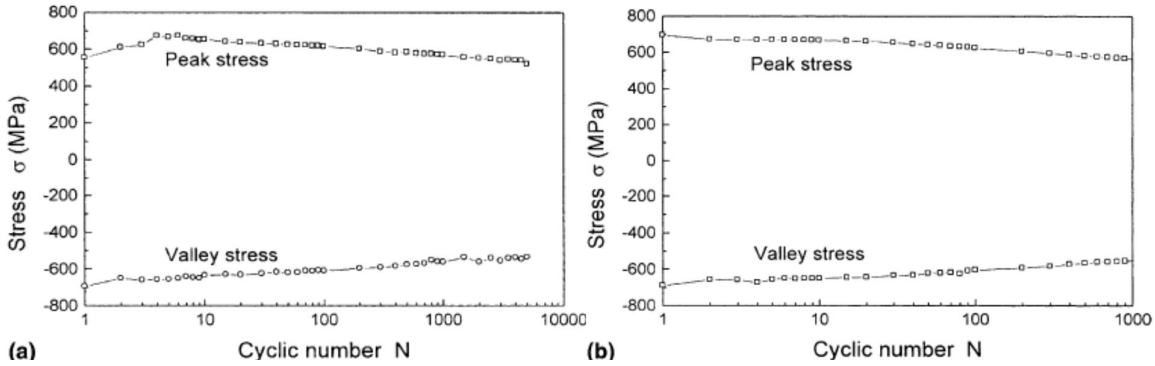

Figure 2.16 Peak and valley stresses vs. cyclic number N with various strain amplitudes: (a) 25CDV4.11, 0.4% (b) 25CDV4.11, 0.6%

When the material show cyclic hardening (i.e., SS304 stainless steel), the ratcheting strain rate decreases with the increase of cycles shown in Fig 2.17,P.C. Lam et.al [21] shown in his experiment initial hardening followed by progressive softening up to failure in case of aluminium-magnesium-silicon alloy. The softening occurred by a progressive decrease in stress for both the tension and compressive parts of a strain amplitude-controlled fatigue test is illustrated in Fig. 2.18.

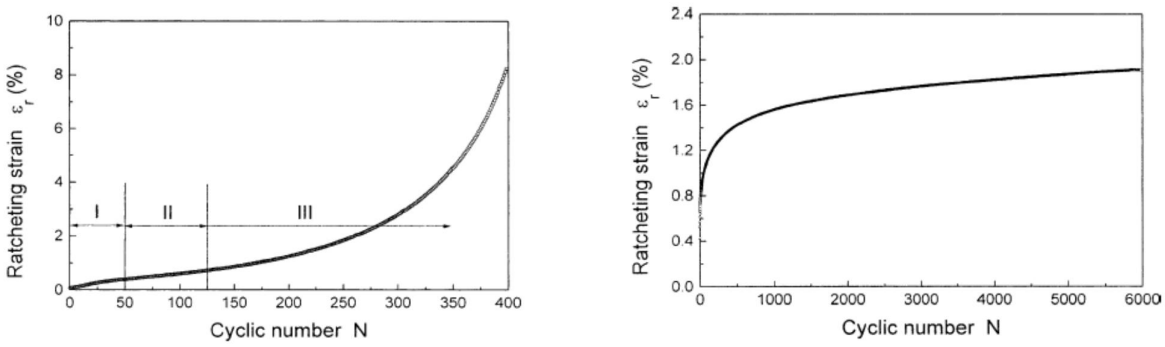

Figure 2.17 Ratcheting strain *vs.* cyclic number N of (a) 25CDV4.11 steel with load condition of 80 ± 600 MPa(b) For SS304 with load condition of 65 ± 260 MPa.

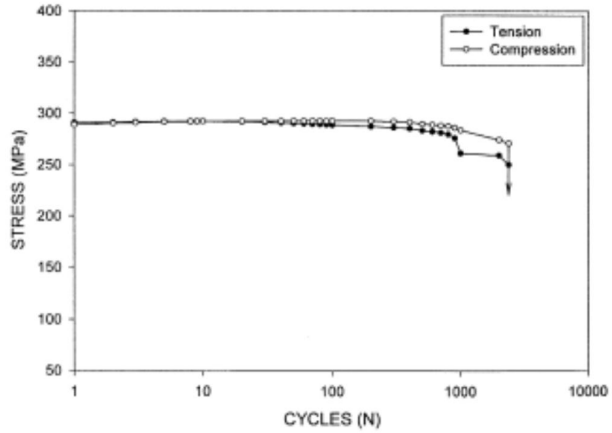

Figure 2.18 Stress response curves showing the variation of tensile stress and compressive stress with cycles at fixed total strain amplitude of 0.60%

2.9.3 Effect of stress rate

Nature of accumulation of ratcheting strain behaviour is same as creep behaviour. There are three stages are in ratcheting as the creep strain development under static load, the primary (transient), secondary (steady-state) and tertiary regions is studied by C. B. Lim et. al. [6].The dependence of ratcheting strain at failure may vary with stress rate and material, the ratcheting strain decreases as the applied stress rate increases (Fig. 2.19).

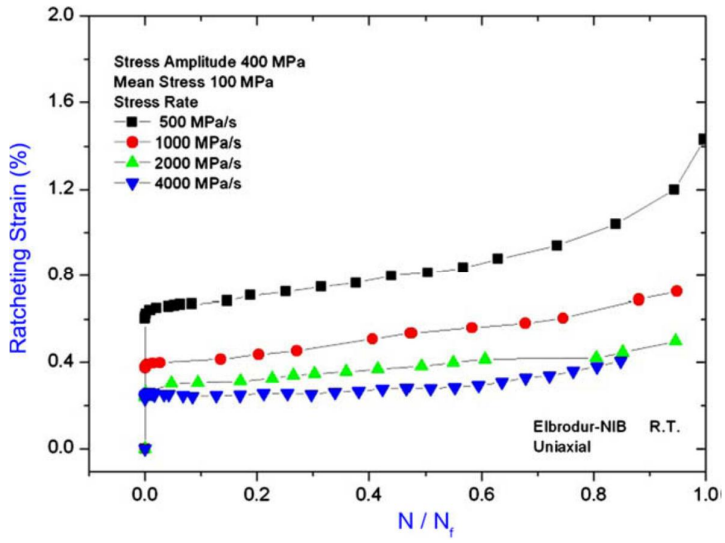

Figure2.19 Ratcheting strain versus cycle at different stress rates for stress amplitude of 400 MPa and mean stress of 100 MPa.

2.10 Materials on which Ratcheting behaviour have been studied

Ratcheting behavior has been studied for cyclic hardening materials like SS304, 316FR and 316L stainless steel and cyclically stable such as U71Mn rail steel and normal carbon steels [9,22,23]. Stress-controlled low cycle fatigue test has been carried out for ASTM A516 Gr 70 steel with tensile mean stress to study the effect of mean stress and ratcheting strain on fatigue life [24]. Lim et. al studied the ratcheting and fatigue behaviour for copper alloy at room temperature with and without σ_m [6]. Ratcheting is also studied for the materials, which are prepared by using powder metallurgy. The cyclic deformation behaviour of two dispersion-strengthened aluminium alloys produced by mechanical alloying is examined. The results of plastic strain-controlled low cycle fatigue tests are compared with those obtained for a conventional A1-Mg alloy (AA5083-H321) and a conventional precipitation-strengthened alloy (AA7075-T6) [25]. The effect of annealing treatment on the ratcheting behaviour and variation in microstructure and monotonic tensile properties is assessed for extruded AZ31B magnesium alloy [26]. Uniaxial ratcheting characteristics of 63Sn/37Pb at room temperature studied experimentally and particular attention is given to ratcheting behaviour under different loading rates. Kang et. al [9], have studied ratcheting behavior of cyclic hardening materials and reported that these materials fail due to combined effect of increasing ratcheting strain and low cycle fatigue, while cyclic softening materials fail under large ratcheting strain. The effect of σ_a, σ_m, loading history and stress ratio on the ratcheting behaviour of high-nitrogen steel was also analyzed [27, 28].

Ratcheting behaviorsô of metals with different crystal structures or values of fault energy was observed by the uniaxial stress-controlled cyclic tension-compression tests with non-zero mean tensile stress [29]. The hysteresis loops for materials having a wavy slip character (high stacking fault energy) are virtually symmetrical with respect to both the stress and strain axes. On the other hand, for materials having a planar slip character (low stacking

fault energy) the loops are always displaced with respect to the strain axis in the direction of the first applied stress. [30, 31]

2.11 Theoretical study on ratcheting

In past years, a series of theoretical studies and modeling on ratcheting have been done [32-37]. All are mentioned that kinematic hardening is the most important mechanism of ratcheting behaviour. It is defined as the hardening of solid due to high stress applied on that solid. A number of constitutive model have been proposed to describe the elasto-plastic behavior under cyclic loading conditions [38].

CHAPTER-3

MATERIAL, EXPERIMENTAL DETAILS AND TESTING PROCEDURES

3.1 Material

The material used for this investigation is SA 508 class 3 low alloy steel. Usually it is used in primary heat transport (PHT) piping systems of reactors for nuclear power plants. SA 508 PHT piping systems conduct cooling operation using D_2O, entering at 249^0C and exiting at 293^0C under 10.5 MPa pressure typically. The steel for this study was available in the form of a pipe with270 mm inner diameter and outer diameter of 320 mm.

3.1.1 Chemical composition

Chemical composition of the investigated material was determined using Optical Emission Spectrometry (OES). For this study, chemical composition of SA 508 steel was obtained through Argonne National Laboratory manual.

3.2Metallography

3.2.1 Specimen Preparation

Samples of approximately 10mm x 10mm x 10mm size were cut from the as received material for metallographic examinations. These samples were first roughly ground on belt grinder. The specimen was made to move perpendicular to the existing scratches on the belt grinder it was continued until the surface is flat and free of nicks, burr etc. after this all corner are chamfer. After rough grinding, the samples were ground with rotating discs of abrasive paper, i.e., wet silicon carbide paper. The coarseness of the paper is indicated by a number. The grinding procedure involves several stages, using a finer paper (higher number) for each successive stage i.e. from 80, 120, 180, 220, 320, 400, 600, 800, 1000, and 1200. Each grinding stage removes the scratches from the previous coarser paper. This was more easily obtained by orienting the specimen perpendicular to the previous scratches, and watching for

these previously oriented scratches to get obliterate. Samples were thoroughly washed with soapy water and then allowed to dry. The final scratch-free surface was obtained by using a rotating wheel (Fig 3.1) covered with a special cloth that was charged with abrasive particles. The abrasive either using diamond paste of particle size of 1εm and 0.25εm or using colloidal suspension of beta alumina having particle size of 0.25εm and 0.1εm. The cloth used in our case was velvet cloth. After fine polishing samples were thoroughly cleaned with soap solution, and subsequently dried using drier. Samples were etched with Kellerôs Reagent [2ml HF (1%), 3ml HCl (1.5%), 5ml HNO3 (2.5%), and 190 ml H2O (95%)]

Figure3.1 Rotating disc for polishing

3.2.2 Optical Microscopy

The polished and etched metallographic specimens were studied using an optical microscope (LEICA DM 2500M (Fig. 3.2)). The software used is LAS V3.6 .These

examinations were carried out in three directions (L-C, L-R, and R-C) at different magnifications and several representative microstructures of the specimens were recorded.

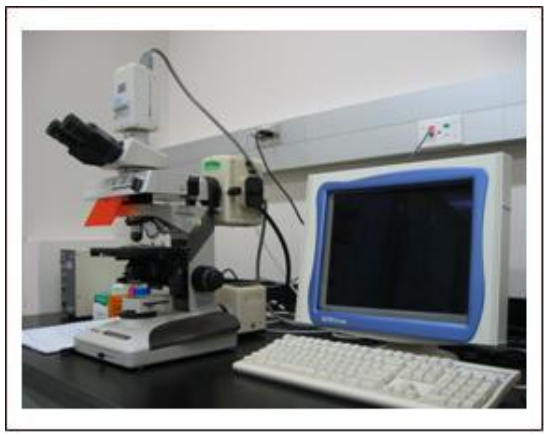

Figure 3.2 Optical Microscope

3.2.3 Grain size measurements

The average grain size of the SA508 steel was determined by the linear intercept method according to ASTM standard E-112 [39]. In this method, a linear test grid was superimposed on the microstructure and the number of grains boundary intercepted by the test line was counted. Such measurements were repeated on 50 randomly chosen fields at a magnification of 500X. The average grain size was then calculated using the relation:

$d = L_T/N_L$ ..... (9)

Where,

N_L = number of grains intercepted by a unit true test line length.

L_T = the true length of a test line is defined as the length of the test line at unit magnification.

3.3 Hardness Determination

The samples prepared for hardness measurements were first made flat and parallel to opposite faces using a belt grinder to ensure precision of measurements. The samples were then mechanically polished using the procedure mentioned in section 3.2. Hardness was evaluated in three directions, viz. L-R, L-C and R-C surfaces, with the help of a Vickers Hardness Tester (Model: Leco LV 700, Fig. 3.3).

Figure 3.3 Leco LV 700 Vickers hardness testers.

The hardness was measured at the load of 30kgf. Minimum3 readings were considered for each sample to calculate the average hardness. The Vickers hardness was calculated using the expression:

$$H_V = \frac{1.854P}{p_{avg}^2} \quad \text{.....10}$$

Where,

P = indentation load.

$D_{avg..} = \frac{d_1 + d_2}{2}$, in which d_1 and d_2 are the lengths of two indentation diagonals.

3.4Tensile Testing

Tensile tests were carried out on cylindrical specimens made from the pipe section such that the loading axis of the specimen is parallel to the longitudinal dimension of the pipe having 5 mm gauge diameter and 30 mm gauge length. The detail drawing of the specimen is shown in Fig. 3.4.

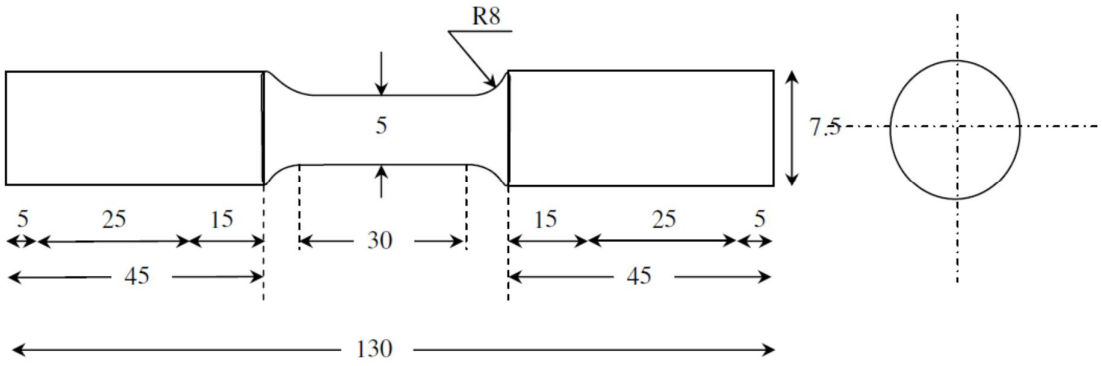

Figure 3.4 Specimen drawing

Tests were done at room temperature using servo electric testing machine with 100KN capacity, under software control. The axial strain was measured by an extensometer of 12.5 gauge length. This extensometer is capable of measuring up to 40% strain. Tensile testswere performed in displacement controlled mode; the strain rate was 1×10^{-3} s^{-1}. During the time of test 800 data points are collected by inbuilt software. The tensile tests were done as per **ASTM E8M** [40] standard.

3.5Uniaxial ratcheting test

The specimens for uniaxial ratcheting test were prepared keeping similar configuration to cylindrical tensile blanks with 7 mm gauge diameter and 13 mm gauge length. Specimens were fabricated from the pipe in such a manner that the loading axis coincides with the pipe axis. Uniaxial ratcheting experiments were carried out at room temperature of 298K using a 100kN servo-electric testing system (Instron, model: 8862, High Wycombe, Buckinghamshire, UK). The system was attached to a computer for test control as well as for data acquisition. All tests were done in true stress control mode till fracture using triangular waveform (Fig. 3.5) at a constant stress rate of 50 MPa/s. Frequency is measured with the help of stress amplitude and fixed during each test.

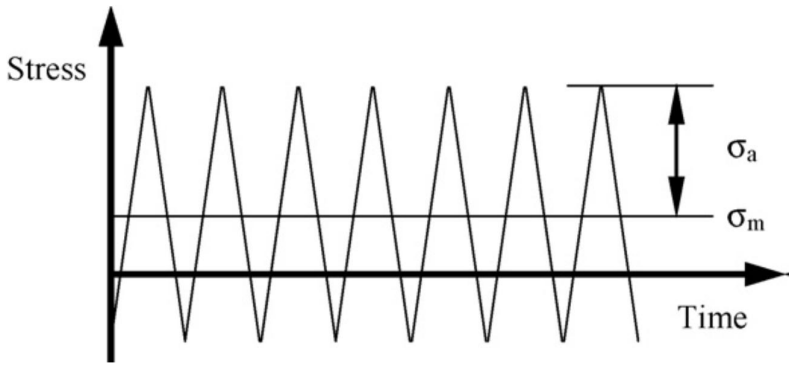

Figure 3.5schematic loading paths for ratcheting test

The tests can be classified into two categories: (i) Constant σ_a with varying σ_m and (ii) constant σ_m with varying σ_a. The combinations of mean stress and stress amplitude were chosen in such a manner that the adopted maximum and minimum stresses fall under tension-compression cycles. A few experiments were also carried out with negative mean stress. The strain measurementsduring cyclic deformations were made using an axial extensometer

having 12.5mm gauge length. Thedata pertaining to stress-extension as well as actuator displacement were continuously recorded; attempts were made to acquire at least 200 data points per cycle for further analyses. The detail drawing of the specimen is shown in Fig. 3.6.

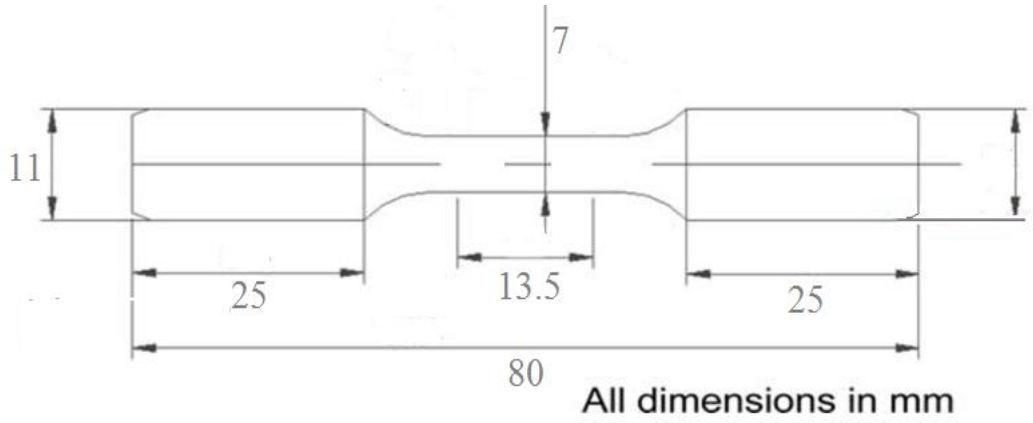

Figure 3.6 Specimen drawing for ratcheting.

3.6Fractography with the SEM (Failure Analysis)

Fractography is the study of fracture surfaces of materials. This method is used to determine the cause of failure in engineering structures by studying the characteristics of a fracture surface. Some modes of crack growth can leave characteristic marks on the surface that identify the mode of crack growth and origin on a macro scale e.g. beach marks or striations on fatigue cracks. Fractography requires examination at a finer scale, which is usually carried out in a Scanning electron microscope or SEM shown in Fig. 3.7.

Figure 3.7 Scanning Electrons Microscope

The resolution of SEM is much higher than the optical microscope, although samples are examined in a partial vacuum at near atmospheric pressures. In general, the propagation of fatigue cracks is strongly controlled to the plane of normal stress and is therefore less dependent upon features of the material. At high stress intensities, striations arranged in bands can be found marking the crack growth during each load cycle. With decreasing stress intensities the striations will disappear and only a weak band structure remains indicating the direction of crack propagation. At very high load pulses as given for instance by a sequence of impacts, the striations can become visible to the naked eye and show a dimple structure in the SEM.

CHAPTER-4

RESULTS & DISCUSSION

4.1 Material characterization

4.1.1 Chemical composition

Chemical composition of steel is given in TABLE 4.1.

Table 4.1 Chemical composition of the SA508 steel

Elements	C	Si	Mn	Ni	Cr	Mo	Cu	Co	V	Fe
Wt%	0.196	0.164	1.4	0.78	0.15	0.446	0.15	0.014	0.013	96.94

4.1.2Micro structural characteristics

The microstructure of the as received SA 508 low alloy steel exhibits nearly equiaxed bainitic grains and few ferrite grains. Ferrite gives ductility and bainite gives strength to the investigated steel. Optical microstructures have been taken in three orientations L-C, L-R, and R-C which are illustrated in Fig. 4.1.

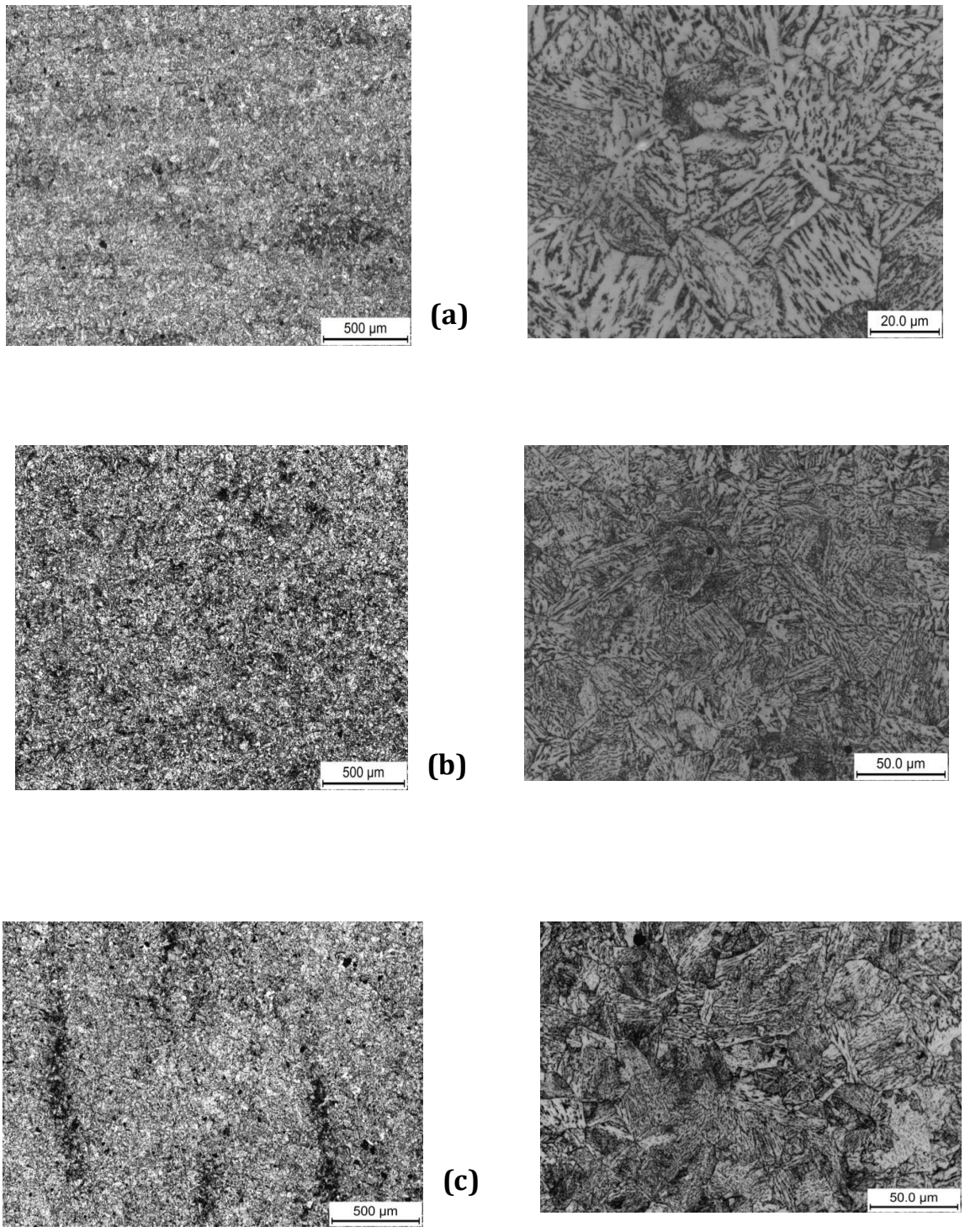

Figure 4.1 Typical optical microstructures of SA 508 steel (a) L-Corientation (b) L-R orientation(c) and R-C Orientation

4.1.3 Grain size measurements

The average grain size of the SA508 steel was determined by the linear intercept method according to ASTM standard E-112 [39]. Linear intercepts are drawn on the microstructure graph of higher magnification. The average grain size is around 20 μm, shown in Fig. 4.2.

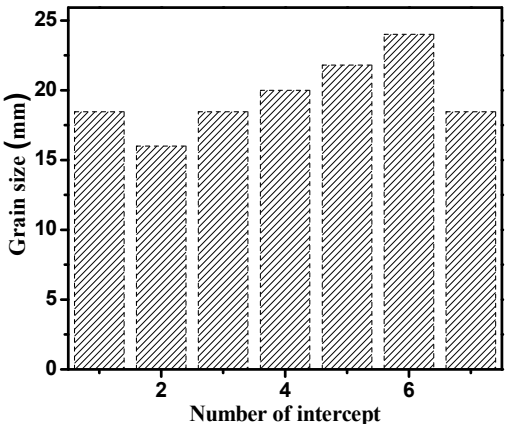

Figure 4.2 Grain Size Distribution

4.1.4 Hardness

Hardness of investigated SA 508 steel samples have been measured in different orientation by Vickers hardness tester. At least three readings have been taken at different positions for a comparative measurement .The results are tabulated in Table 4.2.The dwelling time is 10 s, with applied load of 30kgf.

Table.4.2 Hardness value of SA 508 steel

Direction	Load(kgf)	Hardness(HV)
L-R	30	218.33
L-C	30	223.26
R-C	30	222.8

4.2 Tensile test

Two tensile tests were conducted to check the repeatability of the test results. The engineering stress-strain curve plot is given in Fig. 4.3which shows continuous yielding behavior and the tensile properties given in Table 4.3.Its yield strength has been determined using 0.2% strain offset procedure as suggested in ASTM standard E8M [40].

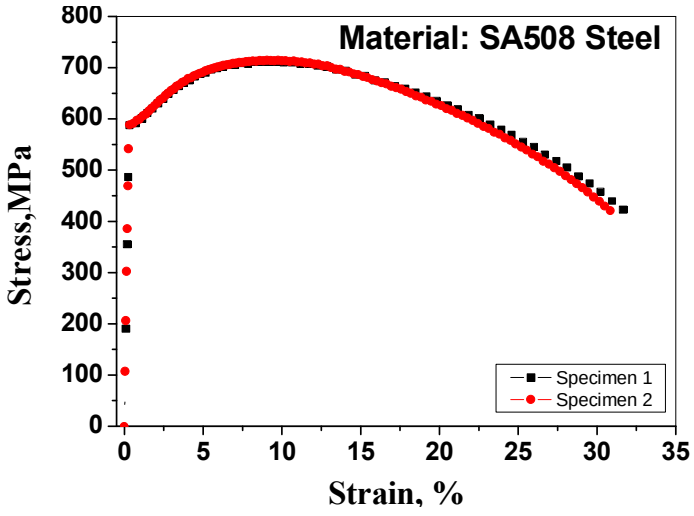

Figure 4.3 Engineering stressï strain behavior of the steel

Table .4.3 Tensile Properties of SA 508 steel

Specimen	YS, MPa	UTS, MPa	% Uniform El	% Total El	% RA
1	584	713	9.23	33.6	66.9
2	588	715	9.6	32.1	66.4

The average of the yield strength of two tests was taken as the basis for determining the mean stress and stress amplitude during ratcheting tests.

4.3 Uniaxial ratcheting behaviour of material

It is understood that variation of strain with stress during cyclic loading produces stress-strain loops known as hysteresis loops. The hysteresis loops those get generated during uniaxial ratcheting experiments shift towards positive or negative plastic strain directions depending on the selection of mean stress. Typical hysteresis loopsthose were obtained during the true stress controlledratcheting test at σ_m = 50MPa, σ_a = 540MPa and σ_m = 50MPa, σ_a = 500MPa are presented in Fig. 4.4 and Fig. 4.5 respectively. In Fig. 4.4 the stress-strain cycles generated up to failure are illustrated whereas only the first two cycles are shown in Fig. 4.5, for clarity. It is clear from the figures that hysteresis loops shifted towards positive strain direction during deformation of ratcheting with positive mean stress.

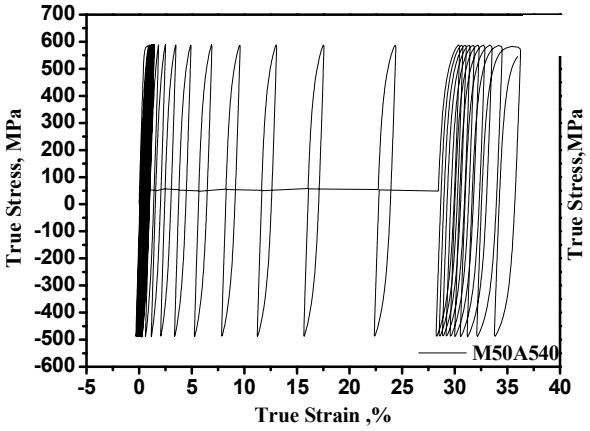

Figure 4.4 Hysteresis loop up to failure for $\mathring{u}_m$= 50 MPa, $\mathring{u}_a$=540MPa.

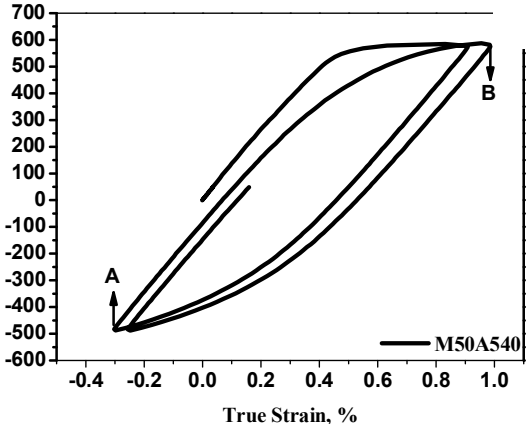

Figure 4.5 Hysteresis loop for 1st and 2nd cycle for $\mathring{u}_m$= 50 MPa, $\mathring{u}_a$=540MPa.

Similar types of hysteresis loops are presented in Fig. 4.6 which are for $\mathring{u}_m$= 50MPa, $\mathring{u}_a$= 500 MPa; (a) representative hysteresis loop of the first cycle, (b) hysteresis loops up to failure. Figure 4.7 represents the hysteresis loops for $\mathring{u}_m$= ï 40MPa, and $\mathring{u}_a$= 520MPa, it is clear from the figure that hysteresis loops shifted towards negative strain direction during deformation of ratcheting with negative mean stress.

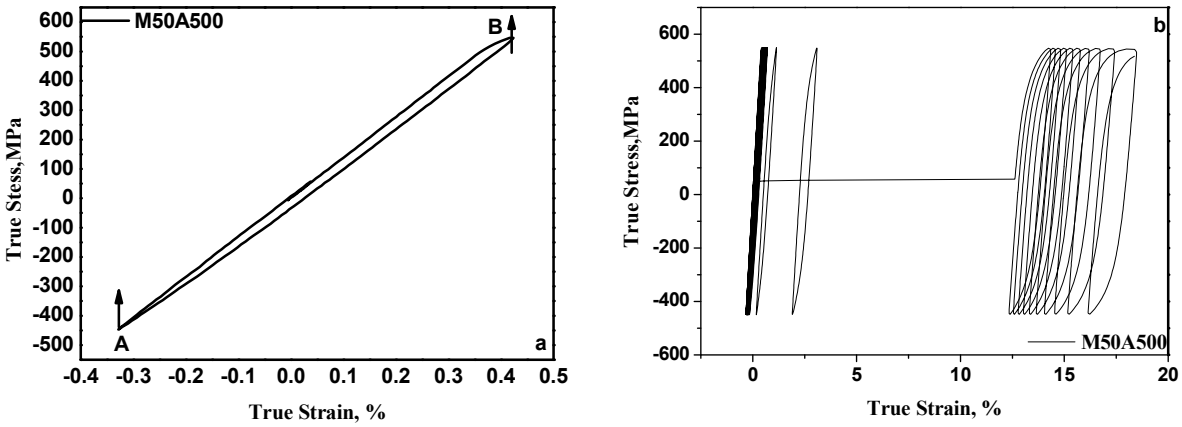

Figure 4.6 Hysteresis loop for first and second cycle (b) hysteresis loops up to failure cycles at $\mathring{u}_m$= 50 MPa, $\mathring{u}_a$=540MPa.

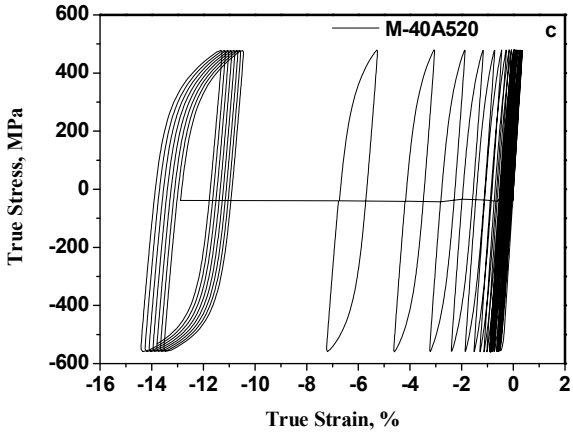

Figure 4.7 Hysteresis loops up to failure cycles at $\mathring{u}_m$= -40MPa, $\mathring{u}_a$= 520 MPa

4.3.1 Effect of stress amplitude on ratcheting strain at constant mean stress.

Variations of accumulated ratcheting strain (Ψ) with number of cycles (N) for constant $\sigma_m$andvarying σ_a are shown in the figure 4.8 (a-c) and the test condition is given in Table. 4.3.

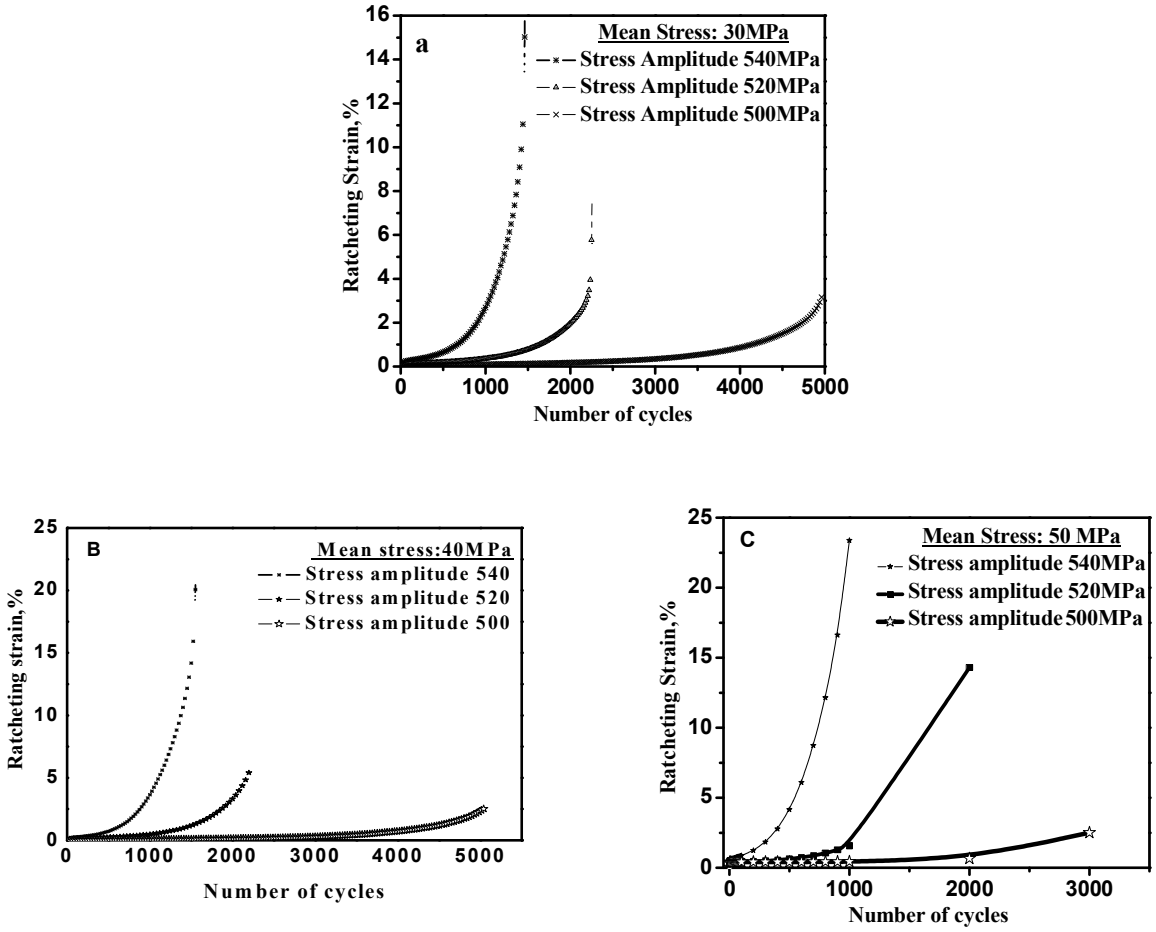

Figure 4.8 Variation of ratcheting strain with number of cycles for varying σ_a and at constant σ_m levels: (a) σ_m = 30 MPa (b) σ_m = 40 MPa, (c) σ_m = 50 MPa

Results in Fig 4.8 show ratcheting strain monotonically increases with increasing number of cycles for any combination of σ_a andσ_m. At any constant σ_m and at any specific N value the

magnitude of $\mathring{U}$ increases with increasing σ_a. For the given result it infers that for increasing ratcheting strain fatigue life (N_f) decreases.

Table 4.4 Selected σ_m and σ_a values for ratcheting tests.

Serial No.	Mean Stress, MPa	Stress Amplitude, MPa		
1	30	540	520	500
2	40	540	520	500
3	50	540	520	500

For example when σ_m and $\sigma_a$are 50 and 500 MPa total strain accumulation is 2.5%, it increases to about 14.3% for σ_a = 520 MPa and about 23.3% for σ_a = 540MPa, at constant σ_m value of 50 MPa. The increase strain accumulation was also observed for mean stress is equal to 30 MPa a 40 MPa in similar fashion. This type of increase in amplitude was also observed for other steel like SA 333 steel [1, 2]., AISI 304LN stainless steel [41] etc.

For understanding the ratcheting behaviour of the SA 508 steel at different combinations of σ_m and σ_a, hysteresis loops obtained during each cycle of the tests were analyzed. Variations in the nature of the hysteresis loops for increasing σ_a are depicted in Fig. 4.9. (a-b). It can be observed from these figures that for a given σ_m level, σ_{max} increases with the increase in σ_a.Thus, it induceshigher plastic strain and also width of the hysteresis loop of any particular number increases with increasing σ_a.

Dutta et al. [41] have reported that increase of ratcheting strain with increasing stress amplitude occurs due to variation in remnant dislocation density. It is wellknown that higher is the dislocation density in a material, higher is the accumulation of plastic strain and vice versa. Hence, it may beinferred that with increasing σ_a for a particular σ_m, total

strainaccumulation will increase because of the increase in the remnantdislocation density. This fact causes increased damage of the material.

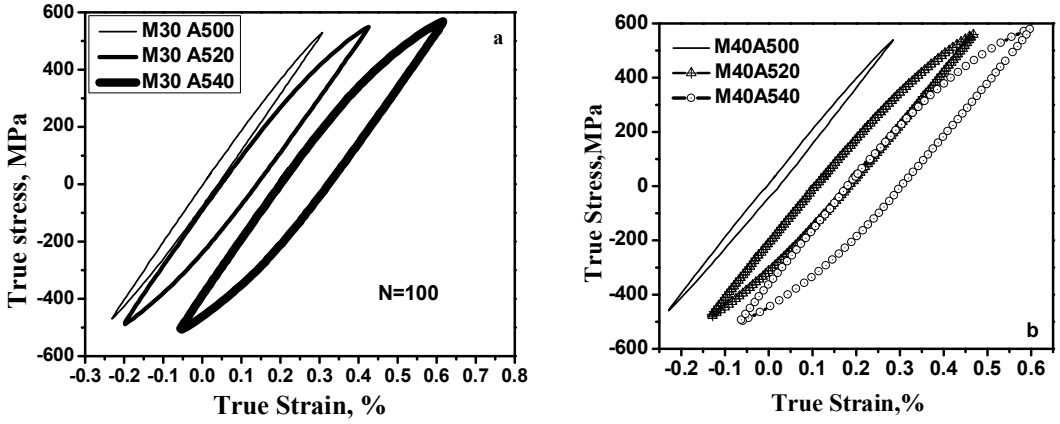

Figure 4.9 Typical stressï strain hysteresis loops showing increased opening of the loops With increasing σ_a at σ_m = 30MPa and 40MPa for N=100.

4.3.2. Effect of mean stress on ratcheting strain at constant stress amplitude

To understand the effect of σ_m on $\dot{U}$ at constant σ_a levels the results is shown in Fig. 4.10, which illustrates that both $\dot{U}$ and N_f increases with increasing σ_m. if we increase the mean stress, ratcheting strain and life both are increases it is clear from figure, one more result is obtain from figure when $\sigma_m$is negative then the accumulated ratcheting strain in compression direction and it is nearly mirror image of same value of positive mean. For example when σ_m and σ_a combination 30 and 520 MPa total strain accumulation is 2.6% it increasing to about 6.03% for σ_m= 40 and about 6.244% for σ_m = -40 MPa.

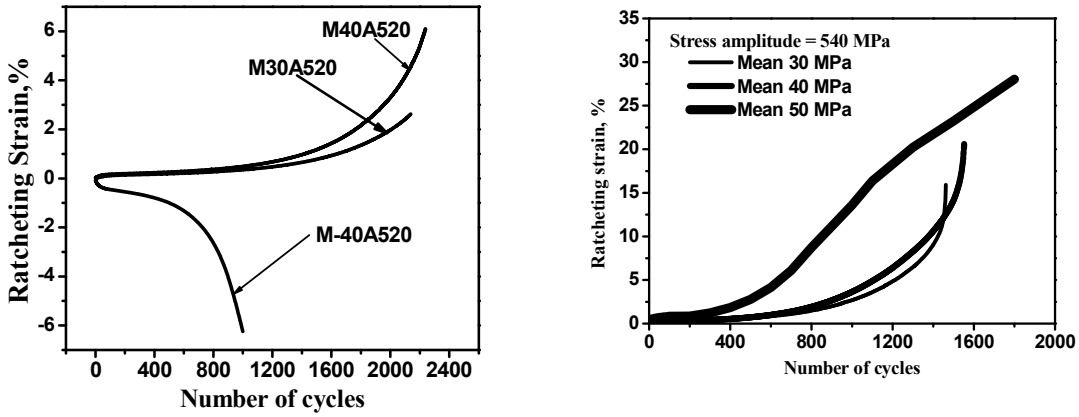

Figure 4.10. (a) Variations of ratcheting strain with number of cycles for varying σ_m and constant σ_a

4.4 Saturation in strain accumulation

To understand the saturation in strain accumulation during ratcheting deformation, the plots between ratcheting strain vs. number of cycles are differentiated, and a new set of graphsare produced. Figure 4.11(a) shows the plot between rate of strain accumulation and number of cycles at σm = 50 MPa and σa= 500 MPa. Similar plots for σm = 50 MPa, σa= 520 MPa and σm = 40 MPa and σa= 520 MPa are given in Fig. 4.11(b) and 4.12. It can observed from all the results that strain accumulation rapidly decreases up to 100 cycles, which slowly attains saturation and finally gets saturated up to 400 cycles. The saturation occurs due to stable nature of dislocation substructure during ratcheting deformation [41].

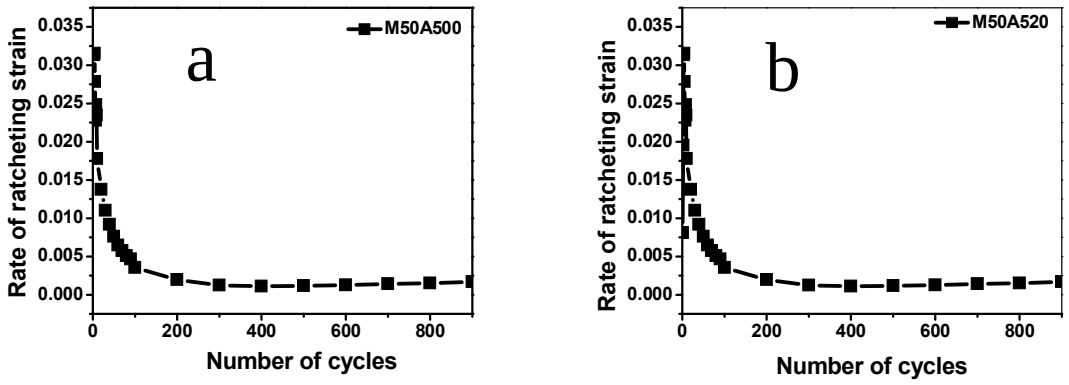

Figure 4.11 Rate of ratcheting strain vs. number of cycles

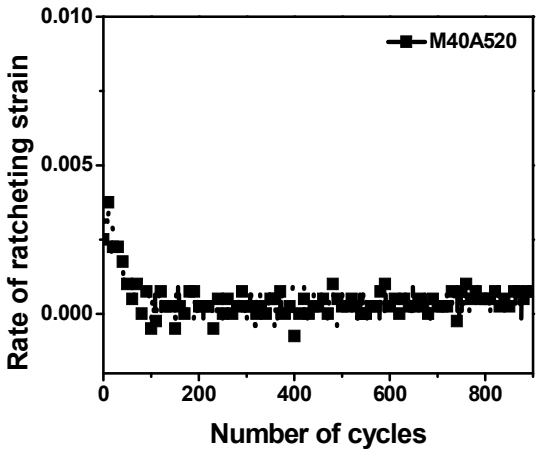

Figure 4.12 Rate of ratcheting strain vs. number of cycles

4.5Fractography

Fracture surfaces of the fatigue testes specimens were studiedusing scanning electron microscope. For this investigation, a set of representative ratcheted specimens which failed during cyclic loading were carefully cut and the fracture surface were examined.This method is usually used to determine the cause of failure in engineering structures by studying the characteristics of a fracture surface. On a microscopic scale, striations can be observed if the fracture is occurred under fatigue. In the present investigation also, striation were observed and typical fractographs are shown in Fig. 4.13(a) and (b). Final failure generally occurs due to overload and can be seen from the fracture surface. Figure 4.13(c) is a representative zone of this type of fracture.

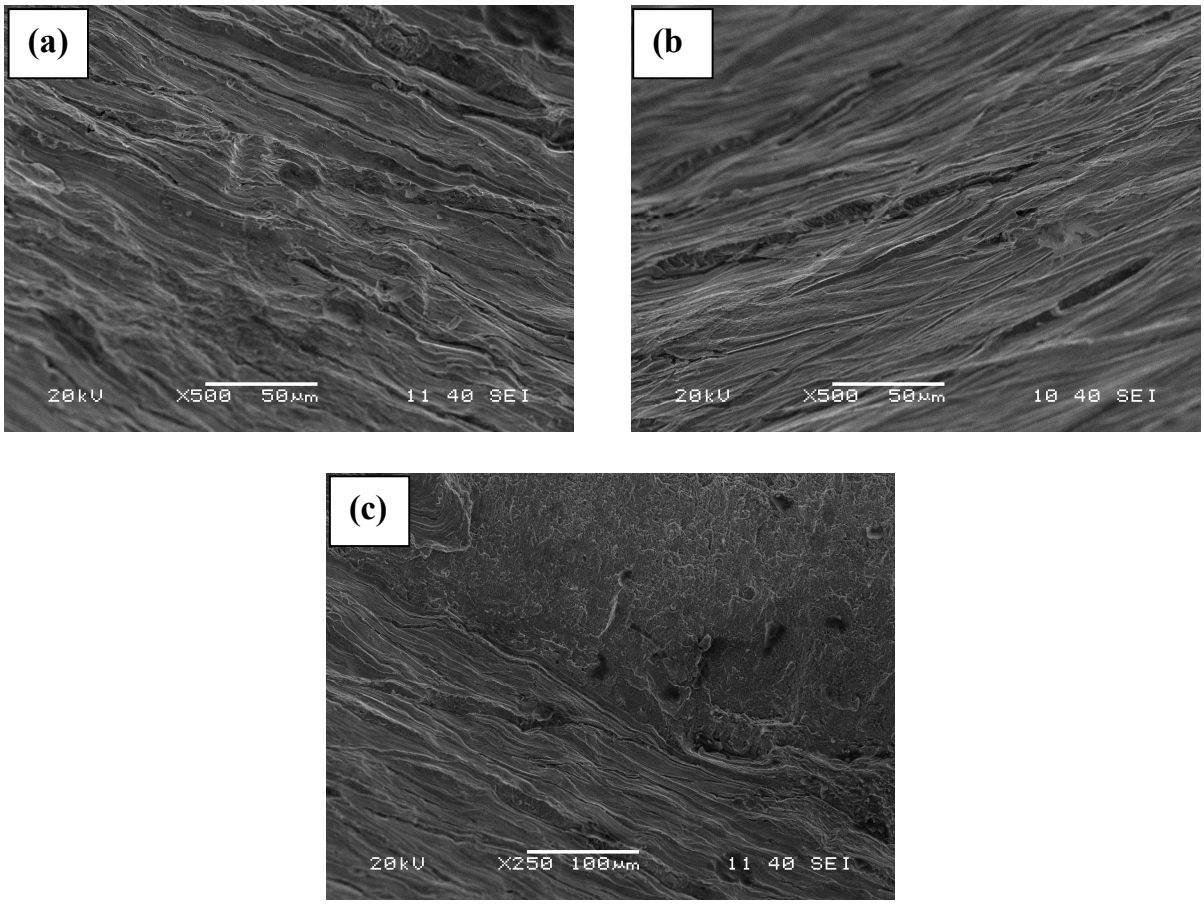

Figure 4.13 Striations formed during cyclic loading (a and b), Interface of overload failure (c).

CHAPTER-5

CONCLUSIONS & FUTURE WORK

5.1 Conclusions

The results and their pertinent analyses related to the present uniaxial ratcheting experiments on SA508 at room temperature assist to infer:

- Accumulation of ratcheting strain can be substantiated from the shifting of hysteresis loops during cyclic loading experiments. The loops shift towards positive strain direction when mean stress is positive; on the other hand opposite nature can be seen for negative mean stress.

- Strain accumulation during ratcheting deformation of the investigated SA508 primary heat transport piping steel increases with increasing stress amplitude at constant mean stress levels. This increase of ratcheting straincan be explained by increase in remnant dislocation density and thereby with increased damage of the material.

- When the stress amplitude is constant, strain accumulation increases with increasing mean stress.Accumulation of ratcheting strain becomes negative, when the mean stress is negative.

- Saturation in strain accumulation is achieved after few cycles due to attainment of stable dislocation configuration after initial 400 cycles.

5.2 Scope for Future Work

The present work leaves a wide scope for future investigation:

- Transmission electron microscopic analyses would be very important scope of experiments to understand the dislocation features responsible for ratcheting behavior of the investigated steel.
- Determination of the effect of pre-straining on the ratcheting behaviour of the materials.
- Ratcheting behavior can be effectively modeled through mathematical simulations. This may be very interesting study for this steel,which is not available in the literature.

CHAPTER-6

REFERENCES

References

I. Dieter G.E., ñMechanical Metallurgyò, McGraw-Hill Book Company, 1988

II. Hertzberg R.W. 1996, Deformation and Fracture Mechanics of Engineering Materials, 4th ed., John Wiley and Sons.

III. Anderson, T.L. Fracture Mechanics: Fundamentals and Applications (CRC Press,1995)

1. Kulkarni SC, Desai YM, Kant T, ñ Uniaxial and biaxial ratchetting study of SA333 Gr.6 steel at room temperatureò International Journal of Pressure Vessels and Piping 80 (2003) 179ï 185.

2. Sivaprasad S, Paul SK, Gupta SK, ñInfluence of uniaxial ratchetting on low cycle fatigue behviour of SA 333 Gr. 6 C-Mn steelò International Journal of Pressure Vessels and Piping 87 (2010) 464-469.

3. Paul SK, Sivaprasad S, Dhar S, Tarafder S, ñRatcheting and low cycle fatigue behavior of SA333 steel and their life predictionò Journal of Nuclear Materials 401 (2010) 17ï 24.

4. Paul SK, Sivaprasad S, Dhar S, Tarafder S. ñCyclic plastic deformation and cyclichardening/softening behavior in 304LN stainless steelò Theoretical and Applied Fracture Mechanics, Theoretical and Applied Fracture Mechanics 54 (2010) 63ï 70

5. Hassan T, Kyriakides S ñRatcheting of cyclically hardening and softening materials, I: uniaxial behaviorò International Journal of Plasticity, 10 (1994) 149-194

6. Lim CB, Kim KS, Seong JB. Ratcheting and fatigue behavior of a copper alloy under uniaxial cyclic loading with mean stress. International Journal of Fatigue, 31 (2009) 501ï 507.

7. Paul SK, Sivaprasad S, Dhar S, Tarafder S, ñTrue stress control asymmetric cyclic plastic behavior in SA333 C-Mn steelò International Journal of Pressure Vessels and Piping, 87 (2010) 440-446.

8. Xia Z, Kujawski D, Ellyin F, ñEffect of mean stress and ratcheting strain on fatigue life of steelò, International Journal of Fatigue, 96 (1995) 335-341.

9. Kang GZ, Li YG, Zhang J, Sun YF, Gao Q ñUniaxial ratcheting and failure behaviors of two steelsò Theoretical and Applied Fracture Mechanics 43 (2005) 199ï 209.

10. Paul SK, Sivaprasad S, Dhar S, Tarafder S ñCyclic plastic deformation behavior in SA333 Gr. 6 Cï Mn steel Materials Science and Engineering A 528 (2011) 7341ï 7349.

11. Gupta C, Chakravartty JK, Reddy GR, Banerjee S, ñUniaxial cyclic deformation behaviour of SA 333 Gr 6 piping steel at room temperatureò, International Journal of Pressure Vessels and Piping, 82 (2005) 459-469.

12. Kang G, Liu Y, Li Z ñExperimental study on ratchetting-fatigue interaction of SS304 stainless steel in uniaxial cyclic stressingò Materials Science and Engineering A 435ï 436 (2006) 396ï 404.

13. Doong SH, Socie DF, Robertson IM, ñDislocation substructures and non proportional hardeningò Journal of Engineering Materials and Technology, 112 (1990) 456-464.

14. Lefebvre D, Ellyin F, ñCyclic response and inelastic strain energy in low cycle fatigueò, International Journal of Fatigue, 6 (1984) 9-15.

15. Satyadevi A, Sivakumar SM, Bhattacharya SS ñA new failure criterion for materials exhibiting ratcheting during very low cycle fatigueò Materials Science and Engineering A 452ï 453 (2007) 380-385.

16. Basaruddin KS, Wooi LC ñUniaxial ratcheting of mild steel under cyclic tensionò Proceedings of International Conference on Applications and Design in Mechanical Engineering (ICADME)11 ï 13 October 2009, BatuFerringhi, Penang, MALAYSIA.

17. Chen G, Chen X, Niu CD, ñUniaxial ratcheting behaviour of 63Sn37Pb solder with loading histories and stress ratesò Materials Science and Engineering A, 421 (2010) 238-244.

18. Ray KK, Dutta K, Shivprasad S, Tarafdar S, ñFatigue damage of AISI304 stainless steel: role of mean stressò, Proceedia Engineering, 2 (2010) 1805-1813.

19. Yang X, ñLow cycle fatigue and cyclic stress ratcheting failure behaviour of carbon steel 45 under uniaxial cyclic loadingò, International Journal of Fatigue, 27 (2005) 1124ï 1132.

20. Chiou YC ñExperimental study of deformation behavior and fatigue life of AISI 304 stainless steel under an asymmetric cyclic loadingò Journal of Marine Science and Technology, 18 (2010) 122-129.

21. Lam P.C., Srivatsan T.S., Hotton B., Al-Hajri M., ñCyclic stress response characteristics of an aluminumï magnesiumï silicon alloyò, Materials Letters, 45 (2000) 186-190.

22. Kang G, Gao Q, ñUniaxial and non-proportionally multiaxial ratcheting of U71Mn rail steel: experiments and simulationsò, Mechanics of Materials, 34 (2002) 809ï 820.

23. Kang GZ, Gao Q, Yang XJ, ñExperimental study on the cyclic deformation and plastic flow of U71Mn rail steelò, International Journal of Mechanical Sciences 44 (8) (2002) 1645ï 1661.

24. Xia Z, Kujawski D, Ellyin F, ñEffect of mean stress and ratcheting strain on fatigue life of steelò, International Journal of Fatigue, 96 (1995) 335-341.

25. Mercer ME, Dickerson SL, Gibeling JC, ñCyclic deformation of dispersion strengthened aluminium alloysò, Materials Science and Engineering A, 203 (1995) 46-58.

26. Zhang XP, Castagne S, Gu CF, Luo XF, ñEffects of annealing treatment on the ratcheting behaviour of extruded AZ31B magnesium alloy under asymmetrical uniaxial cyclic loadingò, Journal of Materials Science, 46 (2011) 1124-1131.

27. Chen G, Shan SC, Chen X, Yuan H, ñRatcheting and fatigue properties of the high-nitrogen steel X13CrMnMoN18-14-3 under cyclic loadingò, Computational Materials Science, 46 (2010) 572ï 578.

28. Tikhovski I, Molders M, Wiemann M, Bingmann D, Fischer A, ñFatigue behaviour and in-vitro biocompatibility of the Ni-free austenitic high-nitrogen steel X13CrMnMoN18-14-3ò, ASTM Committee F04 on Medical and Surgical Materials and Devices, 1438 (2002) 119-136.

29. Kang G, Liu Y, Dong Y, Gao Q, ñUniaxial ratcheting behaviours of metals with different crystal structures or values of fault energy: macroscopic experimentsò, Materials Science and Technology, 27(5) (2010) 453-459.

30. Feltner CE, Laird C, ñCyclic stress strain response of F.C.C. metals and alloys. I. phenomenological experiments and II. dislocation structure and mechanismsò, Acta Metallurgica, 15 (1967) 1621-1653.

31. Pickard AC, Knott JF, ñEffect of testing method on cyclic hardening behaviour in face-centered-cubic alloys, in low cycle fatigue, American Society for Testing and Materials, Philadelphia, PA, (1988): 58-76.

32. Bari S, Hassan T, ñAnatomy of coupled constitutive model for ratcheting simulationò, International Journal of Plasticity, 16 (2000) 381-409.

33. Bari S, Hassan T, ñKinematic hardening rules in uncoupled modelling for multiaxial ratcheting simulationò, International Journal of Plasticity, 17 (2001) 885-905.

34. Chaboche JL, Nouaihas D, ñConstitutive modelling of ratcheting effects. part I experimental facts and properties of classical modelsò, ASME Journals of Engineering Materials and Technology, 3 (1989) 384-390.

35. Armstrong PJ, Frederick CO, ñA mathematical representation of multiaxial Bauschinger effectò, Technical Report RD/B/N731, Berkeley Nuclear Laboratories, (1966).

36. Prager W, ñA new method of analyzing stress and strain in work hardening plastic solidsò, Journal of Applied Mechanics, 23 (1956) 493-496.

37. Ohno N, Wang JD, ñKinematic hardening rules with critical state of dynamic recovery, part II applications to experiments of ratcheting behaviourò, International Journal of Plasticity, 9 (1993) 391-403.

38. Dogui A, Sidoroff F, ñKinematic hardening in large elstoplastic strainò, Engineering Fracture Mechanics, 21 (1985) 685-695.

39. E112, ñStandard test methods for determining grain sizeò, Annual book of ASTM standards, West Conshohocken, PA, 2003.

40. E8M 2009, Standard Test Methods for Tension Testing of Metallic Materials, Annual Book of ASTM Standards, 2009.

41. Dutta K, Sivaprasad S, Tarafder S, Ray KK, ñInfluence of asymmetric cyclic loading on substructure formation and ratcheting fatigue behaviour of AISI 304LN stainless steelò Materials Science and Engineering A 527 (2010) 7571ï 7579.